

1    **The Inflammasome Pathway is Activated by Dengue Virus Non-structural Protein 1 and is**  
2    **Protective During Dengue Virus Infection**

3    Marcus P. Wong<sup>1,2</sup>, Evan Y.W. Juan<sup>1</sup>, Sai S. Chelluri<sup>1</sup>, Phoebe Wang<sup>1</sup>, Felix Pahmeier<sup>1,2</sup>, Bryan  
4    Castillo-Rojas<sup>1</sup>, Sophie F. Blanc<sup>1</sup>, Scott B. Biering<sup>1</sup>, Russell E. Vance<sup>3,4</sup>, Eva Harris<sup>1,2,3</sup>

5    <sup>1</sup> Division of Infectious Diseases and Vaccinology, School of Public Health, University of  
6    California, Berkeley, Berkeley, CA, USA

7    <sup>2</sup> Infectious Diseases and Immunity Graduate Group, School of Public Health, University of  
8    California, Berkeley, Berkeley, CA, USA

9    <sup>3</sup> Division of Immunology and Molecular Medicine, Department of Molecular and Cell Biology  
10   University of California, Berkeley, Berkeley, CA, USA

11   <sup>4</sup> Howard Hughes Medical Institute, University of California, Berkeley, California, USA

12

13

14 **Summary**

15 Dengue virus (DENV) is a medically important flavivirus causing an estimated 50-100 million  
16 dengue cases annually, some of whom progress to severe disease. DENV non-structural protein 1  
17 (NS1) is secreted from infected cells and has been implicated as a major driver of dengue  
18 pathogenesis by inducing endothelial barrier dysfunction. However, less is known about how  
19 DENV NS1 interacts with immune cells and what role these interactions play. Here we report  
20 that DENV NS1 can trigger activation of inflammasomes, a family of cytosolic innate immune  
21 sensors that respond to infectious and noxious stimuli, in mouse and human macrophages.

22 DENV NS1 induces the release of IL-1 $\beta$  in a caspase-1 dependent manner. Additionally, we find  
23 that DENV NS1-induced inflammasome activation is independent of the NLRP3, Pyrin, and  
24 AIM2 inflammasome pathways, but requires CD14. Intriguingly, DENV NS1-induced  
25 inflammasome activation does not induce pyroptosis and rapid cell death; instead, macrophages  
26 maintain cellular viability while releasing IL-1 $\beta$ . Lastly, we show that caspase-1/11-deficient, but  
27 not NLRP3-deficient, mice are more susceptible to lethal DENV infection. Together, these  
28 results indicate that the inflammasome pathway acts as a sensor of DENV NS1 and plays a  
29 protective role during infection.

30

31

32 **Introduction**

33 Dengue virus (DENV) is a mosquito-borne flavivirus consisting of 4 serotypes (DENV1-4) that  
34 represents a growing burden on global public health, with cases increasing 10-fold over the past  
35 20 years. Over 3.8 billion people are at risk of infection with DENV, estimated to reach 6.1  
36 billion by 2080 as urban populations grow and climate change increases the suitable range for  
37 *Aedes* mosquitoes, the transmission vectors for DENV.<sup>1</sup> Of the estimated 105 million people  
38 infected by DENV annually, up to 51 million develop dengue; symptoms span a wide range of  
39 clinical outcomes from an acute febrile illness accompanied by joint and muscle pain to severe  
40 disease characterized by vascular leakage and thrombocytopenia, hemorrhagic manifestations,  
41 pulmonary edema, and hypovolemic shock.<sup>2,3</sup> The causes of endothelial dysfunction and vascular  
42 leak seen in severe dengue disease are likely multifactorial, but some studies suggest a “cytokine  
43 storm” triggered by uncontrolled viral replication and immune activation.<sup>4,5</sup> There are no current  
44 treatment options for severe dengue disease other than supportive care, due in part to an  
45 incomplete understanding of dengue pathogenesis.<sup>6</sup> This underscores a need to better understand  
46 both protective and pathogenic host pathways to develop future therapeutics for dengue.

47 DENV non-structural protein 1 (NS1) has drawn recent interest as a vaccine and therapeutic  
48 target for the prevention of severe dengue. DENV NS1 is an approximately 45-kDa protein that  
49 dimerizes after translation in infected cells.<sup>7</sup> Dimeric, intracellular NS1 associates with the lumen  
50 of the endoplasmic reticulum and participates in the formation of the viral replication complex.<sup>9-</sup>  
51 <sup>11</sup> NS1 is also secreted from infected cells as a tetramer and/or hexamer, with NS1 dimers  
52 oligomerizing around a lipid cargo enriched in triglycerides, cholesteryl esters and  
53 phospholipids.<sup>7,11,12</sup> Secreted NS1 plays multiple roles during infection, including binding and  
54 inactivating complement components and interacting directly with endothelial cells to induce

55 endothelial hyperpermeability and pathogenic vascular leak.<sup>13–17</sup> Mice vaccinated with DENV  
56 NS1 are protected from lethal systemic DENV challenge in mouse models of infection, and  
57 blockade of NS1-induced endothelial hyperpermeability by glycan therapeutics or by NS1-  
58 specific monoclonal antibodies also reduces DENV-induced disease, emphasizing the pivotal  
59 roles NS1 plays in DENV replication and pathogenesis.<sup>14,18–21</sup> DENV NS1 has also been shown  
60 to induce the activation of pro-inflammatory cytokines such as TNF- $\alpha$  and IL-6 in both murine  
61 and human macrophages.<sup>22–25</sup> Studies in mice have identified a TLR4-dependent axis for pro-  
62 inflammatory cytokine induction, and it has been hypothesized that NS1-induced macrophage  
63 activation leads to cytokine storm and immunopathology; however, few studies have  
64 experimentally assessed the mechanisms by which NS1 induces inflammation and whether NS1-  
65 induced inflammation contributes to overall viral pathogenesis.

66 DENV has been shown to trigger multiple innate immune pathways that contribute to both host  
67 defense and pathogenesis.<sup>26,27</sup> Among these pathways are the inflammasomes, a class of innate  
68 immune sensors that surveil the cytosol for a broad range of pathogen or damage-associated  
69 molecular patterns (PAMPs/DAMPs).<sup>28</sup> Canonical inflammasomes recruit the cysteine protease  
70 caspase-1 via the apoptosis-associated speck-like protein containing CARD (ASC) protein.<sup>29</sup>  
71 Certain inflammasomes respond to PAMPs such as viral double-stranded DNA in the case of the  
72 AIM2 inflammasome, or can be triggered by pathogenic effectors; examples include sensing of  
73 viral protease activity by the NLRP1B and CARD8 inflammasomes, sensing of ion fluxes and  
74 membrane damage by the NLRP3 inflammasome, or sensing of toxin-induced Rho guanosine  
75 triphosphatase (Rho GTPase) inactivation by the pyrin inflammasome.<sup>28,30–33</sup> Further, caspase-11  
76 in mice and caspases-4 and -5 in humans can activate the non-canonical inflammasome, in which

77 caspase-11/4/5 binding to lipid A from bacterial lipopolysaccharide (LPS) leads to activation of  
78 the NLRP3 inflammasome.<sup>34,35</sup>

79 Inflammasome signaling typically comprises a two-step process in which inflammasome  
80 components and substrates are first transcriptionally upregulated and/or ‘primed’, usually in  
81 response to PAMPs/DAMPs and nuclear factor- $\kappa$ B (NF- $\kappa$ B) signaling.<sup>28</sup> After priming, a second  
82 stimulus induces inflammasome oligomerization, leading to ASC recruitment and caspase-1  
83 autoproteolytic processing into its active form.<sup>29</sup> The active caspase-1 protease can then cleave  
84 pro-IL-1 $\beta$ , pro-IL-18 and gasdermin D (GSDMD) into their bioactive forms. Cleavage of  
85 GSDMD leads to insertion and oligomerization of the N-terminal domain (GSDMD-NT) to form  
86 pores in the plasma membrane.<sup>36</sup> The formation of GSDMD pores canonically leads to  
87 pyroptosis, a form of inflammatory cell death; however, recent work has shown that GSDMD  
88 pore formation and pyroptosis are distinct events and that macrophages can release IL-1 $\beta$  from  
89 GSDMD pores without undergoing pyroptosis in response to certain stimuli.<sup>37-41</sup> GSDMD pores  
90 also facilitate the release of cleaved IL-1 $\beta$  and IL-18, which then serve as major mediators of  
91 inflammation contributing to host defense as well as driving immunopathology.<sup>37,42</sup> Many viruses  
92 have been shown to activate inflammasomes during infection, including influenza A virus, HIV,  
93 SARS-CoV-2, picornaviruses, and DENV.<sup>27,33,43-45</sup> Inflammasome activation by viruses can be  
94 protective and/or can contribute to pathogenic outcomes.<sup>43,45-48</sup> Ultimately, the impact of  
95 inflammasome activation depends on the context and timing of the infection; thus, understanding  
96 these complexities is crucial for designing inflammasome-targeted therapies as potential  
97 treatments for viral disease.

98 Several studies have begun to investigate whether DENV infection triggers inflammasome  
99 activation and how this might impact DENV pathogenesis. Studies have shown that *in vitro*  
100 DENV infection of mouse and human macrophages, human skin endothelial cells, and platelets,  
101 as well as infection in mice can induce inflammasome activation.<sup>49–54</sup> Clinically, IL-1 $\beta$  levels are  
102 also elevated in dengue patients, implicating a role for inflammasome activation in human  
103 DENV infections.<sup>53,55</sup> Mechanistic studies have implicated both the membrane (M) and NS2A/B  
104 proteins of DENV as viral triggers of the NLRP3 inflammasome.<sup>49,52</sup> *In vivo* studies using an  
105 adeno-associated virus (AAV) vector to induce DENV M expression suggested that DENV M  
106 can cause NLRP3-dependent vascular leak, though the relevance of M-induced inflammasome  
107 activation in DENV infection is unknown.<sup>49</sup> Another study showed that mice treated with an IL-  
108 1 receptor antagonist during DENV infection lost less weight and experienced less vascular leak  
109 compared to untreated controls.<sup>53</sup> Although it is established that DENV infection can induce  
110 inflammasome activation, the viral triggers and the contribution of inflammasome activation  
111 during infection remain open areas of investigation. In this study, we identify secreted NS1 as a  
112 trigger of the inflammasome pathway in a caspase-1-dependent manner that is independent of the  
113 NLRP3, pyrin, and AIM2 inflammasomes but dependent on CD14. Further, we demonstrate that  
114 caspase-1/11 deficiency, but not NLRP3 deficiency, makes mice more susceptible to DENV  
115 infection, indicating that inflammasome activation can be protective during DENV infection.

116

117 **Results**

118 **DENV NS1 can activate the inflammasome pathway**

119 Since DENV NS1 is secreted from infected cells and can activate macrophages to induce a pro-  
120 inflammatory response, we hypothesized that DENV NS1 could be a viral trigger of the

121 inflammasome pathway in macrophages.<sup>22</sup> To test this hypothesis, we assessed whether DENV  
122 NS1 could activate the inflammasome pathway in mouse bone marrow-derived macrophages  
123 (BMDMs). BMDMs were first primed with PAM<sub>3</sub>CSK<sub>4</sub>, a synthetic triacylated lipopeptide  
124 TLR1/TLR2 agonist, and then treated with DENV NS1. Cell supernatants were assessed 24  
125 hours (h) post-treatment for the presence of IL-1 $\beta$  as a readout of inflammasome activation. We  
126 found that DENV NS1 induced the release of IL-1 $\beta$  in BMDMs in a dose-dependent manner  
127 (**Figure 1A**). Additionally, DENV NS1 induced the cleavage of pro-IL-1 $\beta$ , GSDMD, and pro-  
128 caspase-1 into their cleaved, bioactive components (IL-1 $\beta$  p17, GSDMD-N p31, and caspase-1  
129 p20, respectively), confirming activation of the inflammasome pathway (**Figure 1B**). Next, we  
130 obtained BMDMs from mice genetically deficient in caspase-1 and -11, required for canonical  
131 and non-canonical inflammasome signaling, respectively, and compared them to BMDMs from  
132 WT caspase-1/11-sufficient littermates and found that NS1-induced IL-1 $\beta$  release was abolished  
133 in BMDMs derived from caspase-1/11 knockout mice (**Figure 1C**). Similarly, nigericin, a  
134 NLRP3 inflammasome agonist, was unable to induce IL-1 $\beta$  release in caspase-1/1-deficient  
135 macrophages (**Figure 1C**). Consistent with these findings, the caspase-1-specific inhibitor AC-  
136 YVAD-cmk inhibited both DENV NS1 and nigericin-induced IL-1 $\beta$  release in a dose-dependent  
137 manner (**Figure 1D**).<sup>56</sup> Additionally, DENV NS1 was also able to induce cleavage of caspase-1  
138 and the release of bioactive IL-1 $\beta$  in human THP-1-derived macrophages in a caspase-1  
139 dependent manner (**Figure 1E-F**). Collectively, these data suggest that DENV NS1 induces  
140 inflammasome activation in a caspase-1-dependent manner in macrophages.

141

142 **DENV NS1-mediated inflammasome activation is NLRP3-independent.**

143 Since the NLRP3 inflammasome has previously been shown to be activated by other DENV  
144 proteins as well as by NS1 from the closely related Zika virus, we hypothesized that DENV NS1  
145 might also activate the NLRP3 inflammasome.<sup>49,52,57</sup> Surprisingly, we found that DENV NS1  
146 was still able to induce IL-1 $\beta$  cleavage and release in BMDMs derived from *Nlrp3*<sup>-/-</sup> mice,  
147 whereas IL-1 $\beta$  release was severely reduced in BMDMs derived from *Nlrp3*<sup>-/-</sup> mice treated with  
148 the NLRP3 inflammasome activator nigericin (**Figure 2A-B**). Likewise, treatment of WT  
149 BMDMs with the NLRP3-specific inhibitor MCC950 inhibited nigericin-mediated IL-1 $\beta$  release  
150 in a dose-dependent manner, whereas DENV NS1-induced IL-1 $\beta$  release was unaffected by  
151 MCC950 treatment (**Figure 2C**).<sup>58</sup> These data suggest that DENV NS1-mediated inflammasome  
152 activation is independent of the NLRP3 inflammasome. Since IL-1 $\beta$  release downstream of the  
153 non-canonical inflammasome and the lipopolysaccharide (LPS)-triggered inflammasome  
154 pathway requires NLRP3, these results further suggest that NS1-induced inflammasome  
155 activation is not via caspase-11 or due to LPS contamination.<sup>59</sup> We then utilized CRISPR-Cas9  
156 gene editing to knock out additional components in the inflammasome pathway via nucleofection  
157 of Cas9-guide RNA (gRNA) ribonucleoprotein complexes in WT BMDMs to attempt to identify  
158 the inflammasome pathway activated by DENV NS1. We targeted *Nlrp3* (encoding Nlrp3), *Aim2*  
159 (encoding Aim2), *Mefv* (encoding Pyrin) and *Casp1* in C57BL/6 mice using 2 guide RNAs per  
160 gene and used a non-targeting guide (NTG) as an experimental control. This approach achieved  
161 robust deletion of the target proteins, as assessed by Western blot (**Figure 2D**). We then treated  
162 gene-edited BMDMs with DENV NS1 for 48h and assessed inflammasome activation by IL-1 $\beta$   
163 release, as measured by ELISA. Corroborating the results from *Nlrp3*<sup>-/-</sup> mice, CRISPR-Cas9  
164 knockout of *Nlrp3* did not affect DENV NS1-mediated inflammasome activation (**Figure 2E**).  
165 CRISPR-Cas9 knockout of the AIM2 and Pyrin inflammasomes also had no effect on DENV

166 NS1-induced inflammasome activation. Thus, DENV NS1-mediated inflammasome activation in  
167 BMDMs is independent of the NLRP3, AIM2, and Pyrin inflammasomes.

168 **DENV NS1-induced inflammasome activation is dependent on CD14 and does not lead to**  
169 **cell death**

170 We observed that DENV NS1-treated BMDMs maintain their morphology and do not undergo  
171 detectable cell death, in contrast to nigericin-treated cells, despite evidence of cleavage of  
172 GSDMD (**Figure 1B**). Measurement of lactate dehydrogenase (LDH) is often used as a proxy  
173 for pyroptotic cell death; consistent with this, we found that PAM<sub>3</sub>CSK<sub>4</sub>-primed BMDMs treated  
174 with nigericin rapidly released near maximum amounts of LDH 2h post-treatment.<sup>60-62</sup> In  
175 contrast, PAM<sub>3</sub>CSK<sub>4</sub>-primed, NS1-treated BMDMs released LDH at similar levels to the  
176 BMDMs primed with PAM<sub>3</sub>CSK<sub>4</sub> alone, up to 24h post-treatment (**Figure 3A**). In addition, at  
177 24h post-treatment, nigericin-treated macrophages displayed high levels of staining by an amine-  
178 reactive dye used to fluorescently label dead cells, whereas DENV NS1-treated macrophages  
179 were labeled at similar levels to the untreated controls (**Figure 3B**). These lines of evidence  
180 indicate that DENV NS1 induces inflammasome activation without inducing cell death. Previous  
181 studies have shown that pyroptosis and inflammasome activation are separable processes and  
182 that myeloid cells can release IL-1 $\beta$  over time without undergoing pyroptosis.<sup>38,39,41</sup> One such  
183 study showed that oxidized phospholipids can enhance IL-1 $\beta$  release without inducing cell death  
184 through engagement of CD14 in macrophages and dendritic cells.<sup>63</sup> Since DENV NS1 is secreted  
185 from infected cells as an oligomer surrounding a lipid cargo, we hypothesized that DENV NS1  
186 might also enhance IL-1 $\beta$  release by delivering lipids to cells in a CD14-dependent manner.  
187 Indeed, we found that DENV NS1 was able to deplete surface levels of CD14 on BMDMs, as  
188 was LPS, a canonical CD14 ligand, suggesting that DENV NS1 can induce endocytosis of CD14

189 similar to other characterized CD14 ligands (**Figure 3C**). We next generated CD14-deficient  
190 BMDMs by nucleofection (**Figure 3D**) and treated these cells with DENV NS1. We found that  
191 IL-1 $\beta$  release was abrogated in DENV NS1-treated CD14-deficient BMDMs compared to NTG  
192 control cells, suggesting that CD14 is required for DENV NS1 inflammasome activation (**Figure**  
193 **3E**). Nigericin-treated CD14 knockout BMDMs still induced IL-1 $\beta$  release at similar levels to  
194 NTG controls (**Figure 3F**), and CD14-deficient BMDMs were able to secrete TNF- $\alpha$  in response  
195 to PAM<sub>3</sub>CSK<sub>4</sub> (**Figure 3G**), showing that NF- $\kappa$ B responses needed for inflammasome priming  
196 were intact, leading us to conclude that the lack of NS1-triggered inflammasome activation in  
197 CD14-deficient macrophages was not a consequence of off-target effects in other inflammasome  
198 pathways. These findings suggest that DENV NS1 inflammasome activation is CD14-dependent  
199 and induces IL-1 $\beta$  release without pyroptosis.

## 200 **Caspase-1/11 mediates a protective response during DENV infection**

201 We have previously characterized a lethal mouse model of DENV infection and disease  
202 consisting of interferon  $\alpha/\beta$  receptor-deficient (*Ifnar*<sup>-/-</sup>) mice infected with a mouse-adapted  
203 DENV2 strain (D220).<sup>64</sup> To determine how inflammasome activation impacts DENV  
204 pathogenesis upon viral infection, we crossed *Casp1/11*<sup>-/-</sup> or *Nlrp3*<sup>-/-</sup> separately with *Ifnar*<sup>-/-</sup>  
205 mice to generate *Casp1/11*<sup>-/-</sup> x *Ifnar*<sup>-/-</sup> and *Nlrp3*<sup>-/-</sup> x *Ifnar*<sup>-/-</sup> double-deficient mice and infected  
206 them with DENV2 D220. We found that *Casp1/11*<sup>-/-</sup> x *Ifnar*<sup>-/-</sup> mice were significantly more  
207 susceptible to lethal DENV2 infection and showed greater morbidity compared to littermate  
208 controls with functional *Casp1/11* alleles (**Figure 4A-B**), indicating that inflammasome  
209 activation plays a protective role during DENV2 infection in mice. Previous studies have  
210 implicated the NLRP3 inflammasome as playing a pathogenic role during DENV infection; thus,  
211 mice deficient in NLRP3 would be predicted to exhibit less severe disease compared to NLRP3-

212 functional mice. However, we found that *Nlrp3*<sup>-/-</sup> x *Ifnar*<sup>-/-</sup> mice displayed similar outcomes after  
213 lethal DENV2 challenge as littermate controls with functional *Nlrp3* alleles across both high and  
214 low doses of DENV2 D220 (**Figure 4C-D**). Thus, these data suggest that while inflammasomes  
215 can play a protective role during DENV infection, this protection is independent of the NLRP3  
216 inflammasome, consistent with NS1-triggered inflammasome activation patterns that we  
217 measured *in vitro*.

218

219 **Discussion**

220 In this study, we demonstrate that the inflammasome pathway is activated by DENV NS1 in  
221 mouse BMDMs and human THP-1 macrophages. Interestingly, we find that DENV NS1-induced  
222 inflammasome activation is independent of the NLRP3, AIM2 and Pyrin inflammasomes in  
223 BMDMs and that NLRP3 deficiency in mice does not affect the outcome of DENV infection, in  
224 contrast to previous reports ascribing a pathogenic role to the NLRP3 inflammasome during  
225 DENV infection.<sup>49,52</sup> Instead, we find that inflammasome activation may play a protective role  
226 during DENV infection, as caspase-1/11-deficient mice are more susceptible to DENV infection  
227 compared to their caspase-1/11-functional littermates.

228 Our study experimentally assessed the contribution of inflammasome activation to DENV  
229 infection *in vivo* using genetically deficient mice, in contrast to previous studies. In one study,  
230 investigators sought to define the contribution of DENV M to DENV pathogenesis and found  
231 that NLRP3-deficient mice infected with an adeno-associated virus expressing DENV M showed  
232 less pathology than WT controls.<sup>49</sup> However, it is not clear how generalizable this model is to  
233 DENV pathogenesis, as the study relied on expression of DENV M protein by an adeno-  
234 associated virus rather than by infection with DENV. Our study differs in that we use a DENV2

235 strain (D220) in a well-characterized IFNAR-deficient mouse model, which has been previously  
236 shown to more readily model features of DENV pathogenesis observed in severe disease in  
237 humans, such as vascular leak.<sup>64,65</sup> Using this model, we found that caspase-1/11-deficient mice  
238 are more susceptible to DENV infection than their caspase-1/11 functional littermates,  
239 implicating the inflammasome pathway as a protective pathway during DENV infection. Further,  
240 we find that NLRP3-deficient, IFNAR-deficient mice are not protected from lethal DENV  
241 infection and succumb to infection at similar rates as NLRP3-sufficient IFNAR-deficient mice,  
242 thus suggesting that the NLRP3 inflammasome does not contribute to pathogenesis in the context  
243 of DENV infection, at least in our DENV D220 mouse model of vascular leak syndrome.  
244 Another study showed that treatment of mice with IL-1 receptor antagonist can reduce pathology  
245 during DENV infection in IFNAR-deficient mice.<sup>53</sup> Our results do not necessarily conflict with  
246 this prior study since there can be IL-1 $\beta$ -independent effects of inflammasome activation.<sup>66</sup>  
247 Further studies are needed to understand the mechanistic basis of caspase-1/11-mediated  
248 protection during DENV infection.

249 The timing and magnitude of inflammasome activation are key factors in determining whether  
250 activation is protective or detrimental to the host. Administration of the NLRP3 inhibitor  
251 MCC950 at days 1 and 3 after influenza A virus (IAV) infection led to hyper-susceptibility to  
252 lethality, whereas treatment on days 3 and 5 post-infection protected mice against IAV-induced  
253 disease.<sup>48</sup> Thus, in this context, the NLRP3 inflammasome plays both a protective role early in  
254 infection and a pathogenic role later in infection. The use of genetic models in our study  
255 implicates a protective role for inflammasome activation early in DENV infection as well,  
256 though our data does not preclude the possibility of inflammasome activation being pathogenic  
257 in later stages of infection.

258 In addition, increased inflammasome activation was observed under antibody-dependent  
259 enhancement (ADE) conditions during a secondary DENV infection.<sup>67,68</sup> ADE is a phenomenon  
260 whereby cross-reactive non-neutralizing anti-DENV antibodies elicited from a primary DENV  
261 infection facilitate Fc $\gamma$  receptor-mediated viral entry and replication in immune cells during a  
262 secondary DENV infection with a different serotype, resulting in higher viremia and increased  
263 immune activation.<sup>69,70</sup> Thus, the altered viremic and immune context of ADE may also  
264 determine whether inflammasome activation still plays a protective role or contributes to DENV  
265 disease. While our study ascribes a protective role for inflammasome activation during DENV  
266 infection, more investigation is needed to understand whether targeting the inflammasome  
267 pathway at specific times and under ADE conditions can lead to therapeutic benefit during  
268 severe dengue.

269 Our data raises some interesting questions regarding the mechanism of DENV NS1-induced  
270 inflammasome activation. While we establish that DENV NS1 induces inflammasome activation  
271 independently of the NLRP3 inflammasome using multiple orthogonal genetic and chemical  
272 approaches, the identity of the inflammasome activated by DENV NS1 is unknown. CRISPR-  
273 Cas9-mediated knockout of other, well-studied inflammasomes such as Pyrin and AIM2 had no  
274 effect on DENV NS1-induced inflammasome activation, suggesting that these inflammasomes  
275 may not be involved or may be redundant with each other. Further work is needed to establish  
276 whether DENV NS1 may activate other inflammasomes such as NLRP1B, CARD8, NLRP6 and  
277 NLRP10 inflammasomes, as well as to provide deeper insight into the mechanisms behind  
278 inflammasome sensing of DENV NS1 in macrophages.<sup>71,72</sup>

279 Interestingly, we find here that NS1 can activate the inflammasome pathway through a CD14-  
280 dependent pathway without triggering detectable cell death. It has become increasingly  
281 appreciated that inflammasome activation and the formation of GSDMD pores in cell  
282 membranes do not necessarily lead to pyroptotic cell death, but it is unknown how different  
283 inflammasome stimuli induce different cell fates<sup>39</sup>. Previous studies have implicated CD14 as a  
284 receptor for oxidized phospholipids such as 1-palmitoyl-2-glutaryl-sn-glycero-3-phosphocholine  
285 (PGPC) and 1-palmitoyl-2-(5'-oxo-valeroyl)-sn-glycero-3-phosphocholine (POV-PC); these  
286 phospholipids engage CD14 to promote the release of IL-1 $\beta$  from living macrophages via a  
287 pathway dependent on caspase-11, caspase-1 and NLRP3.<sup>40,63,73</sup> We found that, similar to POV-  
288 PC and PGPC, DENV NS1 can deplete CD14 from the surface of macrophages and is dependent  
289 on CD14 to activate the inflammasome pathway. Since LPS is a canonical ligand of CD14 and  
290 cytosolic LPS can activate the non-canonical inflammasome pathway, it was critical to eliminate  
291 the potential role of LPS in our studies. We primed cells with PAM<sub>3</sub>CSK<sub>4</sub> and regularly tested  
292 DENV NS1 stocks for LPS contamination to ensure that LPS exposure was not driving IL-1 $\beta$   
293 release in our experiments. Importantly, non-canonical inflammasome activation by cytosolic  
294 LPS is dependent on the NLRP3 inflammasome, whereas our studies indicate that DENV NS1  
295 activates an inflammasome pathway that is independent of NLRP3. Thus, it is likely that DENV  
296 NS1-induced inflammasome activation is not due to contaminating LPS; rather, we propose that,  
297 like oxidized phospholipids, DENV NS1 utilizes CD14 to induce IL-1 $\beta$  release in macrophages.  
298 However, the mechanism by which oxidized phospholipids enhance IL-1 $\beta$  release remains  
299 poorly understood, and further work will be required to determine whether DENV NS1 operates  
300 via a similar or distinct mechanism.

301 A previous study reported that NS1-associated lipid cargo is enriched in triglycerides, cholesterol,  
302 and phospholipids, lipids commonly found in cell membranes.<sup>11</sup> We speculate that NS1 could act  
303 as a carrier of oxidized phospholipids generated from infected cells and subsequently be detected  
304 by macrophages at sites distal from infection, activating an inflammasome and cytokine response.  
305 We were unable to determine whether oxidized phospholipids were present within the lipid cargo  
306 of our NS1 in this study; however, it would be interesting to explore whether the inflammatory  
307 capacity of NS1 is ultimately modulated by the lipids within the lipid cargo.

308 Overall, our results provide insight into interactions between DENV NS1 and macrophages and  
309 the role of NS1 in protection. Our current study suggests that NS1-myeloid cell interactions can  
310 be protective during DENV infection and that activation of pro-inflammatory circuits during  
311 DENV infection can be beneficial. Thus, we find that the activation of pro-inflammatory  
312 immune responses does not always lead to detrimental outcomes during DENV infection,  
313 contrary to many studies in the field.<sup>22,27,74</sup> Instead, a more nuanced view accounting for the  
314 timing and magnitude of the inflammatory response may be a crucial aspect of understanding  
315 both the beneficial and detrimental aspects of inflammation in DENV infection. Our data suggest  
316 that further investigation into understanding the delicate balance and precise contexts in which  
317 cytokines can be protective and/or pathogenesis during DENV infection will be crucial for  
318 developing novel therapeutics and identifying the best biomarkers to assess risk of progression to  
319 severe disease.

320 **Acknowledgements**

321 We thank Dr. Patrick Mitchell at the University of Washington and Elizabeth Turcotte from Dr.  
322 Russell Vance's laboratory for provision of key reagents and helpful discussions about

323 inflammasome biology. Additionally, we thank Kristen Witt, Dr. Sarah Stanley, and Marietta  
324 Ravesloot-Chavez for training on CRISPR-Cas9 genetic editing in macrophages and access to  
325 their nucleofectors. We also thank Xinyi Feng, Elin Lee, Eduarda Lopes, Pedro Henrique  
326 Nascimento Carneiro da Saliva for assistance with animal colony maintenance and experiments;  
327 Samantha Hernandez, Maria Jose Andrade, Marco Chapa, and Claudia Sanchez San Martin for  
328 administrative and lab management support; and Nicholas Tzuning Lo, Elias Duarte, Sandra Bos,  
329 and P. Robert Beatty for their many helpful discussions. This study was supported by NIH grants  
330 R01 AI124493 and R01 AI168003 to E.H. R.E.V. is an Investigator of the Howard Hughes  
331 Medical Institute. S.B.B was partially supported as an Open Philanthropy Awardee of the Life  
332 Science Research Foundation.

333 **Author Contributions**

334 Conceptualization: M.P.W., S.B.B., R.E.V., and E.H.; Methodology: M.P.W., E.Y.W.J., S.B.B.,  
335 and E.H.; Formal Analysis: M.P.W.; Investigation: M.P.W., E.Y.W.J., S.C.C., P.W., F.P., B.C.R.,  
336 S.F.B., and L.M.D.; Resources: L.M.D., F.T.G.S., L.S.V.B., C.M.R., R.E.V., and E.H.;  
337 Visualization: M.P.W.; Writing-Original Draft: M.P.W., S.B.B., and E.H., Writing-Review and  
338 Editing: M.P.W., E.Y.W.J., S.C.C., F.P., L.M.D., F.T.G.S., C.M.R., S.B.B., R.E.V., and E.H.;  
339 Supervision: S.B.B., R.E.V., and E.H.; Funding Acquisition: E.H.

340 **Declaration of Interests**

341 R.E.V. consults for Ventus Therapeutics and X-biotix Therapeutics.

342

343 **Materials and Methods**

344 **Mice**

345 All mice were bred in-house in compliance with Federal and University regulations. All  
346 experiments involving animals were pre-approved by the Animal Care and Use Committee  
347 (ACUC) of UC Berkeley under protocol AUP-2014-08-6638-2 and maintained under specific  
348 pathogen-free conditions. Wildtype (WT) C57BL/6 mice were obtained from Jackson Labs and  
349 used for preparation of bone marrow-derived macrophage (BMDMs). *Nlrp3*<sup>-/-</sup> and *Casp-1/11*<sup>-/-</sup>  
350 C57BL/6 mice were provided by Dr. Russell Vance and maintained in the Harris lab mouse  
351 colony. *Nlrp3*<sup>+/+</sup> and *Casp 1/11*<sup>+/+</sup> mice were bred to generate the corresponding WT<sup>(+/+)</sup> or  
352 deficient<sup>(-/-)</sup> littermates mice the corresponding<sup>(+/+)</sup> or deficient<sup>(-/-)</sup> littermates mice for all  
353 experiments. For *in vivo* experiments involving DENV2 infection, *Nlrp3*<sup>-/-</sup> and *Casp 1/11*<sup>-/-</sup> were  
354 bred with C57BL/6 mice deficient in the interferon  $\alpha/\beta$  receptor (*Ifnar*<sup>-/-</sup>) to generate doubly-  
355 deficient *Nlrp3*<sup>+/+</sup> x *Ifnar*<sup>-/-</sup> or *Casp-1/11*<sup>+/+</sup> x *Ifnar*<sup>-/-</sup> mice by backcrossing *Nlrp3*<sup>-/-</sup> and *Casp-1/11*<sup>-/-</sup>  
356 mice with *Ifnar*<sup>-/-</sup> mice over 6 generations. The genotypes of mice used for breeding were  
357 tracked via PCR and gel electrophoresis. *Nlrp3*<sup>+/+</sup> x *Ifnar*<sup>-/-</sup> or *Casp-1/11*<sup>+/+</sup> x *Ifnar*<sup>-/-</sup> mice were  
358 bred to generate littermate WT, heterozygous, or KO mice at the *Nlrp3*<sup>-/-</sup> or *Casp-1/11*<sup>-/-</sup> allele.

359 Individual PCR reactions were utilized to confirm the WT genotype and genetically deficient  
360 genotype for *Casp-1/11* and *Nlrp3*. The primers for each of these reactions were as follows:  
361 *Caspase 1/11* WT (CATGCCTGAATAATGATCACC and GAAGAGATGTTACAGAAGCC),  
362 *Caspase 1/11*-deficient (GCGCCTCCCTACCCGG and CTGTGGTACTAACCGATAA), *Nlrp3*  
363 WT (CCACCTGTCTTCTCTCTGGGC and CCTAAGGTAAGCTTTGTCACCCAGG),  
364 *Nlrp3*-deficient (TTCCATTACAGTCACTCCAGATGT and TGCCTGCTTTACTGAAGG). To

365 determine the IFNAR genotype of the mice, a multiplex PCR protocol consisting of three  
366 primers was used (*CGAGGCGAAGTGGTTAAAAG*, *ACGGATCAACCTCATTCCAC*, and  
367 *AATTGCCAATGACAAGACG*).

368 Viral stocks and proteins

369 A mouse-attenuated strain of DENV2, D220, was utilized for infection of *Ifnar*<sup>-/-</sup> mice.<sup>64</sup> The  
370 D220 strain was derived from the Taiwanese DENV2DENV2 isolate PL046 and is a further  
371 modification of the D2S10 strain, as described previously.<sup>64</sup> Viral stocks were titered using  
372 focus-forming assays on Vero cells. All virus stocks were confirmed to be mycoplasma-free.  
373 Recombinant DENV2 NS1 (Thailand/16681/84) was produced in mammalian HEK293 cells or  
374 purchased from The Native Antigen Company (Oxford, UK). All NS1 stocks were certified to be  
375 endotoxin-free and >95% purity.

376 DENV mouse model

377 Six- to eight-week-old littermate mice of either gender were challenged with DENV via  
378 retroorbital intravenous (IV) injection of the indicated plaque-forming units (PFU) of the  
379 DENV2 D220 strain. Mice were observed for morbidity and mortality over a 2-week period.  
380 Morbidity of mice was assessed utilizing a standardized 1-5 scoring system as follows: 1 = no  
381 signs of lethargy, mice are considered healthy; 2 = mild signs of lethargy and fur ruffling; 3 =  
382 hunched posture, further fur ruffling, failure to groom, and intermediate level of lethargy; 4 =  
383 hunched posture with severe lethargy and limited mobility, while still being able to cross the  
384 cage upon stimulation; and 5 = moribund with limited to no mobility and inability to reach food  
385 or water.(REF) Mice scored as 4 were monitored twice per day until recovery or until reaching

386 moribund status. Moribund mice were euthanized immediately. Mice were also weighed to  
387 measure weight changes throughout the infection period.

388 **BMDM generation**

389 BMDMs were generated from 8-13-week-old WT C57BL/6 mice purchased from Jackson  
390 Laboratories or 8-13-week-old C57BL/6 littermate mice of the following genotypes: *Casp-1/11*<sup>-/-</sup>,  
391 *Casp-1/11*<sup>+/+</sup>, *Nlrp3*<sup>-/-</sup>, and *NLRP3*<sup>+/+</sup>. Additionally, BMDMs were generated from 8-13-week-old  
392 WT C57BL/6 mice purchased from Jackson Laboratories. *Nlrp3*<sup>+/+</sup>. Bone marrow was extracted  
393 from the femur and tibia of dissected mice and plated on non-tissue culture-treated 15-cm Petri  
394 dishes at a density of 1 x 10<sup>7</sup> cells per plate in macrophage differentiation medium (DMEM,  
395 Gibco) supplemented with 2mM L-glutamine, 10% fetal bovine serum (FBS; Corning), 1%  
396 penicillin/streptomycin (Pen/Strep, Gibco), and 10% macrophage colony-stimulating factor (M-  
397 CSF) containing supernatant solution harvested from 3T3-CSF cells and cultured at 37°C with  
398 5% CO<sub>2</sub> for 7 days. On day 3 of incubation, cells were supplemented with additional  
399 macrophage differentiation medium. On day 7, differentiated BMDM cells were harvested by  
400 incubating the plated cells in phosphate-buffered saline without calcium and magnesium (PBS)  
401 at 4°C for 20 minutes (min). The BMDM cells were then removed from the plate by gentle  
402 spraying with PBS, resuspended in DMEM supplemented with 1% Pen-Strep, 40% FBS, and  
403 10% DMSO and frozen in liquid nitrogen until future use.

404 **BMDM inflammasome activation assay**

405 A macrophage-based assay was adapted from previously described protocols to assess  
406 inflammasome activation in BMDMs.<sup>60</sup> Frozen BMDMs were thawed and plated in 24-well or  
407 96-well tissue culture-treated, flat-bottom plates in complete DMEM (DMEM + 2mM L-

408 glutamine + 10% FBS + 1% Pen/Strep) at a density of  $1 \times 10^6$  or  $2 \times 10^5$  cells per well, respectively.

409 After plating, cells were left to rest at 37°C and 5% CO<sub>2</sub> overnight. BMDMs were then primed

410 using 1 $\mu$ g/mL Pam<sub>3</sub>CSK<sub>4</sub> (InvivoGen) for 17 hours (h) or left untreated. Primed BMDMs were

411 stimulated with DENV NS1, 5 $\mu$ M nigericin (Invivogen), or left untreated. After 24h,

412 supernatants were spun down at 10,600 x g for 10 minutes, and the cell-free supernatant was

413 collected. BMDM layers were washed twice with PBS and then lysed in RIPA buffer (150mM

414 NaCl, 1% Nonidet P-40, 0.5% sodium deoxycholate, 0.1% sodium dodecyl sulfate (SDS), 50mM

415 Tris pH 7.4) supplemented with protease inhibitor (Roche). Supernatants and cell lysates were

416 stored at -80°C until further analysis. For experiments involving inhibitors, the NLRP3 inhibitor

417 MCC950 (InvivoGen) or caspase-1 inhibitor Ac-YVAD-cmk (InvivoGen) were added at

418 indicated concentrations 30 min prior to treatment with DENV2 NS1 or nigericin.

419 Cell culture

420 HEK-Blue-IL-1 $\beta$  cells were obtained from Invivogen (catalog # hkb-il1b) and grown in complete

421 medium containing DMEM, 10% FBS, 1% Pen/Strep, 100 $\mu$ g/mL Zeocin (Invivogen), and

422 200 $\mu$ g/mL Hygromycin B Gold (Invivogen). WT THP-1 cells or *casp-1*<sup>-/-</sup> THP-1 were

423 purchased from Invivogen and grown in complete medium containing RPMI (Gibco), 10% FBS,

424 and 1% Pen/Strep. HEK-Blue IL-1 $\beta$  reporter cells were grown and assayed in 96-well plates.

425 All cell lines were routinely tested for mycoplasma by PCR kit (ATCC, Manassas, VA).

426

427 THP-1 inflammasome activation assay

428 To assess inflammasome activation in THP-1 macrophages, WT or *casp-1*<sup>-/-</sup> THP-1 human

429 monocytes were differentiated into macrophages in 10ng/mL phorbol 12-myristate 13-acetate

430 (PMA) and primed with medium or 1 $\mu$ g/mL LPS for 4h. Primed macrophages were treated with

431 10 $\mu$ g/mL DENV NS1 or left untreated (LPS only). 18h later, supernatants were collected. Cells  
432 were stimulated with 5 $\mu$ M nigericin for 2h as a positive control. Supernatants were then assessed  
433 for bioactive IL-1 $\beta$  using a HEK-Blue IL-1 $\beta$  reporter assay.

434

435 To assess cleavage of caspase-1 in THP-1 macrophages, WT THP-1 human monocytes were  
436 differentiated into macrophages in 10ng/mL PMA and primed with medium or 100 ng/mL  
437 Pam<sub>3</sub>CSK<sub>4</sub> for 17h. Primed macrophages were then treated with DENV NS1 or 5 $\mu$ M nigericin in  
438 RPMI + 2% FBS + 1% Pen/Strep for 24h. Supernatants were collected, and cells were lysed with  
439 RIPA buffer. Proteins in supernatant were precipitated by methanol/chloroform precipitation and  
440 resuspended in 50uL of 1X SDS-PAGE sample buffer (0.1%  $\beta$ -mercaptoethanol, 0.0005%  
441 bromophenol blue, 10% glycerol, 2% SDS, 63mM Tris-HCl pH 6.8).

442

443 HEK-Blue IL-1 $\beta$  reporter assay

444 To quantify the levels of bioactive IL-1 $\beta$  released from cells, we employed HEK-Blue IL-1 $\beta$   
445 reporter cells. In these cells, binding of IL-1 $\beta$  to the surface receptor IL-1R1 results in the  
446 downstream activation of NF- $\kappa$ B and subsequent production of secreted embryonic alkaline  
447 phosphatase (SEAP) in a dose-dependent manner. SEAP levels were detected using a  
448 colorimetric substrate assay, QUANTI-Blue (Invivogen) by measuring an increase in absorbance  
449 at OD<sub>655</sub>. Culture supernatant from THP-1 cells was added to HEK-Blue IL-1 $\beta$  reporter cells  
450 plated in 96-well format in a total volume of 200  $\mu$ l per well. After 24h, SEAP levels were  
451 assayed by adding 20  $\mu$ l of the supernatant from HEK-Blue IL-1 $\beta$  reporter cells to 180  $\mu$ l of  
452 QUANTI-Blue colorimetric substrate following the manufacturer's protocol. After incubation at  
453 37°C for 30-60 min, absorbance at OD<sub>655</sub> was measured on a microplate reader.

454

455 CRISPR-Cas9-mediated gene editing in primary BMDMs

456 CRISPR-Cas9 gene editing was performed in WT BMDMs to knock out specified genes using a  
457 nucleofection-based approach.<sup>75</sup> Bone marrow from WT B6 mice was isolated, and cells were  
458 differentiated as previously described. On day 5 of macrophage differentiation, BMDMs were  
459 harvested and resuspended in P3 Primary Cell Nucleofector Solution with Supplement (Lonza).  
460 Separately, Cas9-ribonuclear protein (RNP) complexes were made by incubating *S. pyogenes*  
461 Cas9 with 2 nuclear localization signals (SpCas9-2NLS, Synthego) and 2 guide RNAs per gene  
462 (Synthego), together with Alt-R<sup>TM</sup> Cas9 Electroporation Enhancer (IDT) at room temperature for  
463 25 min. BMDMs (4x10<sup>6</sup> per gene target) were mixed with RNP complex, and cells were  
464 nucleofected in 16-well Nucleocuvette strips (Lonza) using a 4D-Nucelofector<sup>®</sup> (Lonza).  
465 Nucleofected cells were then seeded in non-tissue culture-treated 15-cm Petri dishes in  
466 macrophage differentiation medium and differentiated for an additional 5 days, with medium  
467 changes every 2 days. After differentiation, gene-edited macrophages were harvested and used in  
468 the previously described inflammasome activation assay. Gene-edited macrophages were  
469 stimulated with inflammasome activators for 48h before supernatants were assessed for IL-1 $\beta$ .  
470 Additionally, primed, gene-edited macrophages were lysed in RIPA buffer, and cell lysates were  
471 frozen for validation of efficient gene knockout by Western blot.

472 Cytokine and lactate dehydrogenase (LDH) quantification

473 Cytokine levels in cell supernatants were assessed using the mouse IL-1 $\beta$ /IL-1F2 DuoSet ELISA  
474 kit (R&D Systems) and mouse TNF- $\alpha$  DuoSet ELISA kit (R&D Systems) according to the  
475 manufacturer's instructions. ELISA plates were measured at OD<sub>450</sub> using a microplate reader,  
476 and cytokine levels were quantified by interpolation using a standard curve. Supernatants were

477 assayed for LDH release immediately after stimulation time courses per the manufacturer's  
478 protocol from the CytoTox 96<sup>®</sup> Non-Radioactive Cytotoxicity Assay (Promega). Measurements  
479 of absorbance readings were performed on a microplate reader at wavelengths of 490 nm and  
480 680 nm. LDH release was assessed as a percentage of background-subtracted maximum LDH  
481 values from lysed cells.

482 SDS-PAGE and Western blot

483 Cell supernatants and lysates were diluted in 6X SDS-PAGE protein sample buffer (360mM Tris  
484 pH 6.8, 12% SDS, 18%  $\beta$ -mercaptoethanol, 60% glycerol, 0.015% bromophenol blue), boiled for  
485 10 min at 95°C, and resolved using SDS-PAGE. The proteins were then transferred onto a  
486 nitrocellulose membrane, washed 3 times with Tris-buffered saline with 0.1% Tween20 (TBS-T)  
487 and probed with primary antibodies diluted in 5% non-fat dry milk in TBS-T at 4°C overnight.  
488 The membrane was then washed 3 times with TBS-T and probed with secondary antibodies in  
489 5% non-fat dry milk in TBS-T rocking at room temperature for 2 hours. The membrane was then  
490 washed 3 times with TBS-T and 2 times in TBS and developed using SuperSignal West Pico  
491 PLUS Chemiluminescence reagent (ThermoFisher). The resulting membrane was imaged on a  
492 BioRad ChemiDoc system and visualized using Image Lab software (BioRad). The antibodies  
493 and working dilutions used were as follows: goat- $\alpha$ -mouse IL-1 $\beta$ , 1:1000 (R&D Systems, AF-  
494 401-NA); rabbit- $\alpha$ -NLRP3, 1:1000 (Cell Signaling, D4D8T); rabbit- $\alpha$ -mouse AIM2, 1:500 (Cell  
495 Signaling, 63660),  $\alpha$ -mouse Caspase-1 (p20) 1:1000 (Adipogen, Casper-1),  $\alpha$ -human Caspase-1  
496 (p20), 1:1000 (Adipogen, Bally-1);  $\alpha$ -Pyrin, 1:1000 (Abcam, EPR18676); goat- $\alpha$ -mouse IgG  
497 HRP, 1:5000 (Biolegend, 405306); donkey- $\alpha$ -rabbit IgG HRP, 1:5000 (Biolegend, 405306);  $\alpha$ -  
498 actin HRP, 1:2000 (Santa Cruz Biotechnologies, sc-8432).

499

500 Flow Cytometry

501 BMDMs were primed with 1 $\mu$ g/mL Pam<sub>3</sub>CSK<sub>4</sub> for 17h, then stimulated with 5 $\mu$ g/mL *E. coli* LPS,  
502 10 $\mu$ g/mL DENV NS1, or 5 $\mu$ M nigericin for the indicated time periods at 37°C. Cells were  
503 washed twice with PBS, then incubated in PBS at 4°C for 10 min and scraped to suspend cells.  
504 Suspended cells were stained with either Live/Dead Fixable Far Red Stain (ThermoFisher) or  
505 APC- $\alpha$ -mouse CD14 primary antibody (clone Sa2-8; Thermo Scientific) on ice in the dark for 30  
506 minutes. Purified rat  $\alpha$ -mouse CD16/CD32 (Mouse FcBlock; Becton Dickenson) was used as the  
507 blocking reagent to reduce non-specific binding of the antibodies. The stained cells were then  
508 washed twice with 1ml cold FACS buffer (1% Bovine Serum Albumin [Sigma] and 1% Purified  
509 Mouse IgG [Invitrogen] in PBS) and fixed in 500 $\mu$ L of 4% paraformaldehyde at room  
510 temperature. Cells were washed once in PBS and kept in 500 $\mu$ L PBS at 4°C in the dark until  
511 analysis with an Intellicyt iQue3 Screener (Sartorius). For viability analysis, a dead-cell gate was  
512 set based on unstained cell controls, and the percentage of singlet cells in the dead-cell gate  
513 compared to all singlet cells was calculated. For CD14 expression, the mean fluorescence  
514 intensity (MFI) of CD14 from unstimulated or stimulated cells was recorded. The percentage of  
515 surface receptor staining at 30 min, which is the ratio of the MFI values measured from the  
516 stimulated cells to those measured from the unstimulated cells, was plotted to reflect the  
517 efficiency of receptor endocytosis. At least 10,000 events were acquired per sample for analysis.

518 Statistics

519 All quantitative analyses were conducted and all data were plotted using GraphPad Prism 8  
520 Software. Data with error bars are represented as mean  $\pm$  SEM. Statistical significance for  
521 experiments with more than two groups was tested with two-way ANOVA with multiple  
522 comparison test correction as indicated.

524 **Figure Legends**

525 **Figure 1. DENV NS1 can activate the inflammasome.**

526 **(A)** BMDMs were primed with PAM<sub>3</sub>CSK<sub>4</sub> (1 $\mu$ g/mL) for 17 h and then treated with DENV2  
527 NS1 at indicated concentrations, treated with 5 $\mu$ M nigericin, or left untreated (PAM only). IL-1 $\beta$   
528 levels in the supernatant after 2h (nigericin) or 24h (NS1 and PAM only) were measured by  
529 ELISA. \*p<0.05 as determined by one-way ANOVA with Dunn's multiple comparison  
530 correction. **(B)** Representative Western blots of BMDM cell lysates after priming with  
531 PAM<sub>3</sub>CSK<sub>4</sub> (1 $\mu$ g/mL) for 17h and treatment with 10 $\mu$ g/mL DENV2 NS1 (DENV NS1) or  
532 PAM<sub>3</sub>CSK<sub>4</sub> treatment for 24h without NS1 treatment (PAM only). **(C)** WT and *Casp1/11*<sup>-/-</sup>  
533 BMDMs were primed with PAM<sub>3</sub>CSK<sub>4</sub> (1 $\mu$ g/mL) for 17h and then treated with DENV2 NS1 at  
534 the indicated concentrations, nigericin (5 $\mu$ M), or medium (PAM only). IL-1 $\beta$  levels in the  
535 supernatant after 2h (Nigericin) or 24h (NS1 and PAM only) were measured by ELISA. \*p<0.05,  
536 \*\*p<0.01. Statistical significance was determined using two-way ANOVA followed by multiple  
537 t-tests using Holm-Sidak correction. **(D)** BMDMs were primed with PAM<sub>3</sub>CSK<sub>4</sub> (1 $\mu$ g/mL) for  
538 17h and then pre-treated with Ac-YVAD-cmk at the indicated concentrations before addition of  
539 DENV2 NS1 (10 $\mu$ g/mL), nigericin (5 $\mu$ M), or medium (Inhibitor only). IL-1 $\beta$  levels in  
540 supernatant 2h (Nigericin) or 24h (NS1 and PAM only) were measured by ELISA. **(E)** WT or  
541 *Casp-1*<sup>-/-</sup> THP-1 human monocytes were differentiated into macrophages in 10ng/mL PMA and  
542 primed with medium or LPS for 4h. Primed macrophages were treated with DENV NS1  
543 (10 $\mu$ g/mL) or left untreated (LPS only). Eighteen hours later, supernatants were collected. Cells  
544 were stimulated with 5 $\mu$ M nigericin for 2h as a positive control. Bioactive IL-1 $\beta$  in supernatants  
545 was measured using HEK-Blue IL-1R reporter cells. **(F)** Representative Western blots of THP-1  
546 macrophage cell lysates after priming with PAM<sub>3</sub>CSK<sub>4</sub> (100ng/mL) for 17h and treatment with  
547 DENV2 NS1 at indicated concentrations ( $\mu$ g/mL), treatment with 5 $\mu$ M nigericin, or no treatment

548 for 24h. The data are shown as the mean  $\pm$  standard deviation (SD) of 3 independent experiments  
549 (A, C-D) or 4-6 independent experiments (E) or a representative image taken from 2 biological  
550 replicates (B,F).

551 **Figure 2. DENV NS1-induced inflammasome activation is NLPR3-independent.**

552 (A) WT and *Nlrp3*<sup>-/-</sup> BMDMs were primed with PAM<sub>3</sub>CSK<sub>4</sub> (1 $\mu$ g/mL) for 17h and then treated  
553 with DENV2 NS1 at indicated concentrations, nigericin (5 $\mu$ M), or medium (PAM only). IL-1 $\beta$   
554 levels in supernatant 2h (nigericin) or 24h (NS1 and PAM only) were measured by ELISA.  
555 \*p<0.05, \*\*p<0.01. Statistical significance was determined using two-way ANOVA followed by  
556 multiple t-tests with Holm-Sidak correction. (B) Representative Western blots of cell lysates  
557 from WT and *Nlrp3*<sup>-/-</sup> BMDMs after priming with PAM<sub>3</sub>CSK<sub>4</sub> (1 $\mu$ g/mL) for 17h and treatment  
558 with DENV2 NS1 (10 or 5  $\mu$ g/mL), treatment with nigericin (5 $\mu$ M), or no treatment for 24h. (C)  
559 BMDMs were primed with PAM<sub>3</sub>CSK<sub>4</sub> (1 $\mu$ g/mL) for 17h and then pre-treated with MCC950 at  
560 the indicated concentrations before addition of DENV2 NS1 (10 $\mu$ g/mL), nigericin (5 $\mu$ M), or  
561 medium (Inhibitor only). IL-1 $\beta$  levels in the supernatant after 2h (Nigericin) or 24h (NS1 and  
562 PAM only) were measured by ELISA. (D) Representative Western blots of cell lysates from  
563 BMDMs nucleofected with Cas9-gRNA ribonuclear protein complexes to knock out the  
564 indicated genes. Two gRNAs per gene were used per nucleofection. NTG = non-targeting guide.  
565 (E) Knockout BMDMs from (D) were primed with PAM<sub>3</sub>CSK<sub>4</sub> (1 $\mu$ g/mL) for 17h and treated  
566 with DENV2 NS1 (10 $\mu$ g/mL) or left untreated for 48h. \*p<0.05. Statistical significance was  
567 determined using two-way ANOVA followed by multiple t-tests with Holm-Sidak correction.  
568 The data are shown as the mean  $\pm$  SD of 3 biological replicates (A,C), a representative image  
569 taken from 2 biological replicates (B,D), or data pooled from 5 independent experiments with 3  
570 biological replicates per guide (E).

571 **Figure 3. DENV NS1 induces inflammasome activation in macrophages in a CD14-  
572 dependent manner without inducing cell death.**

573 **(A-B)** BMDMs were primed with PAM<sub>3</sub>CSK<sub>4</sub> (1 $\mu$ g/mL) for 17h and then treated with DENV2  
574 NS1 (10 $\mu$ g/mL), nigericin (5 $\mu$ M), or medium (PAM only). **(A)** At the indicated timepoints,  
575 supernatants were assessed for lactase dehydrogenase (LDH) levels as a proxy for cell death.  
576 LDH levels were calculated as a percentage of maximum LDH release. **(B)** Cells were stained  
577 using a LIVE/DEAD Fixable Far Red stain and analyzed by flow cytometry. \*p<0.05 \*\*p<0.01  
578 \*\*\*p<0.001. Statistical significance was determined using two-way ANOVA with Dunnett's  
579 multiple comparison test. **(C)** BMDMs were primed with PAM<sub>3</sub>CSK<sub>4</sub> (1 $\mu$ g/mL) for 17h and then  
580 treated with DENV2 NS1 (10 $\mu$ g/mL), LPS (5 $\mu$ g/mL) or no treatment (Untreated). After 30 min,  
581 cells were stained for surface CD14 expression and analyzed by flow cytometry. Data are  
582 normalized as a percentage of the median fluorescence intensity of the treatment groups divided  
583 by the untreated control. \*\*p<0.01. Statistical significance was determined using one-way  
584 ANOVA with Holm-Sidak's multiple comparisons test. **(D)** Representative Western blots of cell  
585 lysates from BMDMs nucleofected with either NTG or CD14 Cas9-gRNA ribonuclear protein  
586 complexes. **(E-G)** BMDMs from **(D)** were primed with PAM<sub>3</sub>CSK<sub>4</sub> (1 $\mu$ g/mL) for 17h and  
587 treated with DENV2 NS1 (10 $\mu$ g/mL), nigericin (5 $\mu$ M) or no treatment for 48h. IL-1 $\beta$  levels in  
588 supernatant after 24h (Nigericin) or 48h (NS1 and PAM only) were measured by ELISA **(E-F)**.  
589 TNF- $\alpha$  levels were measured in supernatants 17h post-priming with PAM<sub>3</sub>CSK<sub>4</sub> **(G)**.  
590 \*\*\*p<0.001. Statistical significance was determined using two-way ANOVA with Sidak's  
591 multiple comparison test. The data are shown as the mean  $\pm$  SD of 3 biological replicates  
592 (A,C,E), 5 biological replicates (B), or 2 biological replicates (F-G) or a representative image  
593 taken from 2 biological replicates (D).

594

595 **Figure 4. The inflammasome is protective during DENV infection.**

596 **(A-B)** Survival curves **(A)** and weight loss over time **(B)** of *Casp1/11*<sup>+/+</sup>*Ifnar*<sup>-/-</sup> (Caspase 1/11

597 WT), *Casp1/11*<sup>+/+</sup>*Ifnar*<sup>-/-</sup> (Caspase 1/11 Het), or *Casp1/11*<sup>-/-</sup>*Ifnar*<sup>-/-</sup> (Caspase 1/11 KO)

598 littermates infected intravenously with  $3 \times 10^5$  PFU of DENV2 D220. Survival was monitored

599 over 14 days. Weight loss was monitored over 9 days. Numbers in parentheses indicate the

600 numbers of mice in each group. \*\*p<0.01. Statistical significance was determined by Mantel–

601 Cox log-rank test **(A)** or two-way ANOVA with Holm-Sidak's multiple comparisons test **(B)**.

602 **(C-D)** Survival curves of *Nlrp3*<sup>+/+</sup>*Ifnar*<sup>-/-</sup> (NLRP3 WT), *Nlrp3*<sup>+/+</sup>*Ifnar*<sup>-/-</sup> (NLRP3 Het), or *Nlrp3*

603 <sup>-/-</sup>*Ifnar*<sup>-/-</sup> (NLRP3 KO) littermates infected intravenously with a  $5 \times 10^5$  PFU (High Dose) **(C)** or

604  $7.5 \times 10^4$  PFU (Low Dose) **(D)** of DENV2 D220 and monitored over 10 days. Numbers in

605 parentheses indicate the numbers of mice in each group.

606 **References**

- 607 1. Messina, J.P., Brady, O.J., Golding, N., Kraemer, M.U.G., Wint, G.R.W., Ray, S.E., Pigott, D.M., Shearer, F.M., Johnson, K., Earl, L., et al. (2019). The current and future global distribution and population at risk of dengue. *Nat. Microbiol.* *4*, 1508–1515. 10.1038/s41564-019-0476-8.
- 611 2. Cattarino, L., Rodriguez-Barraquer, I., Imai, N., Cummings, D.A.T., and Ferguson, N.M. (2020). Mapping global variation in dengue transmission intensity. *Sci. Transl. Med.* *12*. 10.1126/scitranslmed.aax4144.
- 614 3. World Health Organization (2009). *Dengue guidelines for diagnosis, treatment, prevention and control*□: new edition (World Health Organization).
- 616 4. Aguilar-Briseño, J.A., Moser, J., and Rodenhuis-Zybert, I.A. (2020). Understanding 617 immunopathology of severe dengue: lessons learnt from sepsis. *Curr. Opin. Virol.* *43*, 41–49. 10.1016/j.coviro.2020.07.010.
- 619 5. Srikiatkachorn, A., Mathew, A., and Rothman, A.L. (2017). Immune Mediated Cytokine 620 Storm and Its Role in Severe Dengue. *Semin. Immunopathol.* *39*, 563–574. 10.1007/s00281-017-0625-1.
- 622 6. Wong, J.M., Adams, L.E., Durbin, A.P., Muñoz-Jordán, J.L., Poehling, K.A., Sánchez- 623 González, L.M., Volkman, H.R., and Paz-Bailey, G. (2022). Dengue: A Growing Problem 624 With New Interventions. *Pediatrics* *149*, e2021055522. 10.1542/peds.2021-055522.
- 625 7. Flamand, M., Megret, F., Mathieu, M., Lepault, J., Rey, F.A., and Deubel, V. (1999). 626 Dengue virus type 1 nonstructural glycoprotein NS1 is secreted from mammalian cells as a 627 soluble hexamer in a glycosylation-dependent fashion. *J. Virol.* *73*, 6104–6110.
- 628 8. Welsch, S., Miller, S., Romero-Brey, I., Merz, A., Bleck, C.K.E., Walther, P., Fuller, S.D., 629 Antony, C., Krijnse-Locker, J., and Bartenschlager, R. (2009). Composition and Three- 630 Dimensional Architecture of the Dengue Virus Replication and Assembly Sites. *Cell Host 631 Microbe* *5*, 365–375. 10.1016/j.chom.2009.03.007.
- 632 9. Płaszczyca, A., Scaturro, P., Neufeldt, C.J., Cortese, M., Cerikan, B., Ferla, S., Brancale, A., 633 Pichlmair, A., and Bartenschlager, R. (2019). A novel interaction between dengue virus 634 nonstructural protein 1 and the NS4A-2K-4B precursor is required for viral RNA replication 635 but not for formation of the membranous replication organelle. *PLoS Pathog.* *15*, e1007736. 636 10.1371/journal.ppat.1007736.
- 637 10. Glasner, D.R., Puerta-Guardo, H., Beatty, P.R., and Harris, E. (2018). The Good, the Bad, 638 and the Shocking: The Multiple Roles of Dengue Virus Nonstructural Protein 1 in Protection 639 and Pathogenesis. *Annu. Rev. Virol.* *5*, 227–253. 10.1146/annurev-virology-101416-041848.
- 640 11. Gutsche, I., Coulibaly, F., Voss, J.E., Salmon, J., d'Alayer, J., Ermonval, M., Larquet, E., 641 Charneau, P., Krey, T., Mégret, F., et al. (2011). Secreted dengue virus nonstructural protein

- 642 NS1 is an atypical barrel-shaped high-density lipoprotein. *Proc. Natl. Acad. Sci. U. S. A.* **108**,  
643 8003–8008. 10.1073/pnas.1017338108.
- 644 12. Shu, B., Ooi, J.S.G., Tan, A.W.K., Ng, T.-S., Dejnirattisai, W., Mongkolsapaya, J.,  
645 Fibriansah, G., Shi, J., Kostyuchenko, V.A., Screamton, G.R., et al. (2022). CryoEM structures  
646 of the multimeric secreted NS1, a major factor for dengue hemorrhagic fever. *Nat. Commun.*  
647 **13**, 6756. 10.1038/s41467-022-34415-1.
- 648 13. Avirutnan, P., Fuchs, A., Hauhart, R.E., Somnuke, P., Youn, S., Diamond, M.S., and  
649 Atkinson, J.P. (2010). Antagonism of the complement component C4 by flavivirus  
650 nonstructural protein NS1. *J. Exp. Med.* **207**, 793–806. 10.1084/jem.20092545.
- 651 14. Beatty, P.R., Puerta-Guardo, H., Killingbeck, S.S., Glasner, D.R., Hopkins, K., and Harris, E.  
652 (2015). Dengue virus NS1 triggers endothelial permeability and vascular leak that is  
653 prevented by NS1 vaccination. *Sci. Transl. Med.* **7**, 304ra141-304ra141.  
654 10.1126/scitranslmed.aaa3787.
- 655 15. Puerta-Guardo, H., Glasner, D.R., and Harris, E. (2016). Dengue Virus NS1 Disrupts the  
656 Endothelial Glycocalyx, Leading to Hyperpermeability. *PLoS Pathog.* **12**, e1005738.  
657 10.1371/journal.ppat.1005738.
- 658 16. Glasner, D.R., Ratnasiri, K., Puerta-Guardo, H., Espinosa, D.A., Beatty, P.R., and Harris, E.  
659 (2017). Dengue virus NS1 cytokine-independent vascular leak is dependent on endothelial  
660 glycocalyx components. *PLOS Pathog.* **13**, e1006673. 10.1371/journal.ppat.1006673.
- 661 17. Barbachano-Guerrero, A., Endy, T.P., and King, C.A. (2020). Dengue virus non-structural  
662 protein 1 activates the p38 MAPK pathway to decrease barrier integrity in primary human  
663 endothelial cells. *J. Gen. Virol.* **101**, 484–496. 10.1099/jgv.0.001401.
- 664 18. Modhiran, N., Gandhi, N.S., Wimmer, N., Cheung, S., Stacey, K., Young, P.R., Ferro, V.,  
665 and Watterson, D. (2019). Dual targeting of dengue virus virions and NS1 protein with the  
666 heparan sulfate mimic PG545. *Antiviral Res.* **168**, 121–127. 10.1016/j.antiviral.2019.05.004.
- 667 19. Sousa, F.T.G. de, Biering, S.B., Patel, T.S., Blanc, S.F., Camelini, C.M., Venzke, D., Nunes,  
668 R.J., Romano, C.M., Beatty, P.R., Sabino, E.C., et al. (2022). Sulfated  $\beta$ -glucan from  
669 *Agaricus subrufescens* inhibits flavivirus infection and nonstructural protein 1-mediated  
670 pathogenesis. *Antiviral Res.* **203**, 105330. 10.1016/j.antiviral.2022.105330.
- 671 20. Biering, S.B., Akey, D.L., Wong, M.P., Brown, W.C., Lo, N.T.N., Puerta-Guardo, H.,  
672 Tramontini Gomes de Sousa, F., Wang, C., Konwerski, J.R., Espinosa, D.A., et al. (2021).  
673 Structural basis for antibody inhibition of flavivirus NS1–triggered endothelial dysfunction.  
674 *Science* **371**, 194–200. 10.1126/science.abc0476.
- 675 21. Modhiran, N., Song, H., Liu, L., Bletchly, C., Brillault, L., Amarilla, A.A., Xu, X., Qi, J.,  
676 Chai, Y., Cheung, S.T.M., et al. (2021). A broadly protective antibody that targets the  
677 flavivirus NS1 protein. *Science* **371**, 190–194. 10.1126/science.abb9425.

- 678 22. Modhiran, N., Watterson, D., Muller, D.A., Panetta, A.K., Sester, D.P., Liu, L., Hume, D.A.,  
679 Stacey, K.J., and Young, P.R. (2015). Dengue virus NS1 protein activates cells via Toll-like  
680 receptor 4 and disrupts endothelial cell monolayer integrity. *Sci. Transl. Med.* *7*, 304ra142.  
681 10.1126/scitranslmed.aaa3863.
- 682 23. Modhiran, N., Watterson, D., Blumenthal, A., Baxter, A.G., Young, P.R., and Stacey, K.J.  
683 (2017). Dengue virus NS1 protein activates immune cells via TLR4 but not TLR2 or TLR6.  
684 *Immunol. Cell Biol.* *95*, 491–495. 10.1038/icb.2017.5.
- 685 24. Chan, K.W.K., Watanabe, S., Jin, J.Y., Pompon, J., Teng, D., Alonso, S., Vijaykrishna, D.,  
686 Halstead, S.B., Marzinek, J.K., Bond, P.J., et al. (2019). A T164S mutation in the dengue  
687 virus NS1 protein is associated with greater disease severity in mice. *Sci. Transl. Med.* *11*,  
688 eaat7726. 10.1126/scitranslmed.aat7726.
- 689 25. Benfrid, S., Park, K.-H., Dellarole, M., Voss, J.E., Tamietti, C., Pehau-Arnaudet, G., Raynal,  
690 B., Brûlé, S., England, P., Zhang, X., et al. (2022). Dengue virus NS1 protein conveys pro-  
691 inflammatory signals by docking onto high-density lipoproteins. *EMBO Rep.* *23*, e53600.  
692 10.15252/embr.202153600.
- 693 26. Uno, N., and Ross, T.M. (2018). Dengue virus and the host innate immune response. *Emerg.*  
694 *Microbes Infect.* *7*, 167. 10.1038/s41426-018-0168-0.
- 695 27. Shrivastava, G., Valenzuela Leon, P.C., and Calvo, E. (2020). Inflammasome Fuels Dengue  
696 Severity. *Front. Cell. Infect. Microbiol.* *10*, 489. 10.3389/fcimb.2020.00489.
- 697 28. Barnett, K.C., Li, S., Liang, K., and Ting, J.P.-Y. (2023). A 360° view of the inflammasome:  
698 Mechanisms of activation, cell death, and diseases. *Cell* *186*, 2288–2312.  
699 10.1016/j.cell.2023.04.025.
- 700 29. Lu, A., Magupalli, V.G., Ruan, J., Yin, Q., Atianand, M.K., Vos, M.R., Schröder, G.F.,  
701 Fitzgerald, K.A., Wu, H., and Egelman, E.H. (2014). Unified Polymerization Mechanism for  
702 the Assembly of ASC-Dependent Inflammasomes. *Cell* *156*, 1193–1206.  
703 10.1016/j.cell.2014.02.008.
- 704 30. Zhao, Y., Yang, J., Shi, J., Gong, Y.-N., Lu, Q., Xu, H., Liu, L., and Shao, F. (2011). The  
705 NLRC4 inflammasome receptors for bacterial flagellin and type III secretion apparatus.  
706 *Nature* *477*, 596–600. 10.1038/nature10510.
- 707 31. Hornung, V., Ablasser, A., Charrel-Dennis, M., Bauernfeind, F., Horvath, G., Caffrey, D.R.,  
708 Latz, E., and Fitzgerald, K.A. (2009). AIM2 recognizes cytosolic dsDNA and forms a  
709 caspase-1-activating inflammasome with ASC. *Nature* *458*, 514–518. 10.1038/nature07725.
- 710 32. Sandstrom, A., Mitchell, P.S., Goers, L., Mu, E.W., Lesser, C.F., and Vance, R.E. (2019).  
711 Functional degradation: A mechanism of NLRP1 inflammasome activation by diverse  
712 pathogen enzymes. *Science* *364*, eaau1330. 10.1126/science.aau1330.

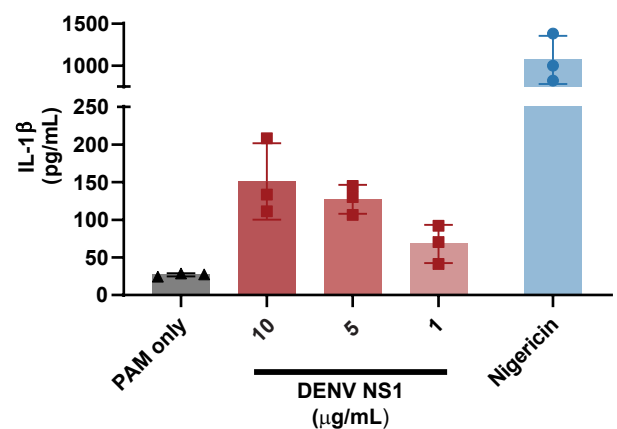
- 713 33. Tsu, B.V., Beierschmitt, C., Ryan, A.P., Agarwal, R., Mitchell, P.S., and Daugherty, M.D.  
714 (2021). Diverse viral proteases activate the NLRP1 inflammasome. *eLife* *10*, e60609.  
715 10.7554/eLife.60609.
- 716 34. Hagar, J.A., Powell, D.A., Aachoui, Y., Ernst, R.K., and Miao, E.A. (2013). Cytoplasmic  
717 LPS activates caspase-11: implications in TLR4-independent endotoxic shock. *Science* *341*,  
718 1250–1253. 10.1126/science.1240988.
- 719 35. Kayagaki, N., Wong, M.T., Stowe, I.B., Ramani, S.R., Gonzalez, L.C., Akashi-Takamura, S.,  
720 Miyake, K., Zhang, J., Lee, W.P., Muszyński, A., et al. (2013). Noncanonical inflammasome  
721 activation by intracellular LPS independent of TLR4. *Science* *341*, 1246–1249.  
722 10.1126/science.1240248.
- 723 36. Sims, J.E., and Smith, D.E. (2010). The IL-1 family: regulators of immunity. *Nat. Rev.  
724 Immunol.* *10*, 89–102. 10.1038/nri2691.
- 725 37. Liu, X., Zhang, Z., Ruan, J., Pan, Y., Magupalli, V.G., Wu, H., and Lieberman, J. (2016).  
726 Inflammasome-activated gasdermin D causes pyroptosis by forming membrane pores.  
727 *Nature* *535*, 153–158. 10.1038/nature18629.
- 728 38. Kayagaki, N., Kornfeld, O.S., Lee, B.L., Stowe, I.B., O'Rourke, K., Li, Q., Sandoval, W.,  
729 Yan, D., Kang, J., Xu, M., et al. (2021). NINJ1 mediates plasma membrane rupture during  
730 lytic cell death. *Nature* *591*, 131–136. 10.1038/s41586-021-03218-7.
- 731 39. Evavold, C.L., Ruan, J., Tan, Y., Xia, S., Wu, H., and Kagan, J.C. (2018). The Pore-Forming  
732 Protein Gasdermin D Regulates Interleukin-1 Secretion from Living Macrophages. *Immunity*  
733 *48*, 35–44.e6. 10.1016/j.jimmuni.2017.11.013.
- 734 40. Zanoni, I., Tan, Y., Di Gioia, M., Broggi, A., Ruan, J., Shi, J., Donado, C.A., Shao, F., Wu,  
735 H., Springstead, J.R., et al. (2016). An endogenous caspase-11 ligand elicits interleukin-1  
736 release from living dendritic cells. *Science* *352*, 1232–1236. 10.1126/science.aaf3036.
- 737 41. de Sá, K.S.G., Amaral, L.A., Rodrigues, T.S., Ishimoto, A.Y., de Andrade, W.A.C., de  
738 Almeida, L., Freitas-Castro, F., Batah, S.S., Oliveira, S.C., Pastorello, M.T., et al. (2023).  
739 Gasdermin-D activation promotes NLRP3 activation and host resistance to *Leishmania*  
740 infection. *Nat. Commun.* *14*, 1049. 10.1038/s41467-023-36626-6.
- 741 42. Heilig, R., Dick, M.S., Sborgi, L., Meunier, E., Hiller, S., and Broz, P. (2018). The  
742 Gasdermin-D pore acts as a conduit for IL-1 $\beta$  secretion in mice. *Eur. J. Immunol.* *48*, 584–  
743 592. 10.1002/eji.201747404.
- 744 43. Sarvestani, S.T., and McAuley, J.L. (2017). The role of the NLRP3 inflammasome in  
745 regulation of antiviral responses to influenza A virus infection. *Antiviral Res.* *148*, 32–42.  
746 10.1016/j.antiviral.2017.10.020.
- 747 44. Wang, Q., Gao, H., Clark, K.M., Mugisha, C.S., Davis, K., Tang, J.P., Harlan, G.H., DeSelm,  
748 C.J., Presti, R.M., Kutluay, S.B., et al. (2021). CARD8 is an inflammasome sensor for HIV-1  
749 protease activity. *Science* *371*, eabe1707. 10.1126/science.abe1707.

- 750 45. Diamond, M.S., and Kanneganti, T.-D. (2022). Innate immunity: the first line of defense  
751 against SARS-CoV-2. *Nat. Immunol.* *23*, 165–176. 10.1038/s41590-021-01091-0.
- 752 46. Thomas, P.G., Dash, P., Aldridge, J.R., Ellebedy, A.H., Reynolds, C., Funk, A.J., Martin,  
753 W.J., Lamkanfi, M., Webby, R.J., Boyd, K.L., et al. (2009). NLRP3  
754 (NALP3/CIAS1/Cryopyrin) mediates key innate and healing responses to influenza A virus  
755 via the regulation of caspase-1. *Immunity* *30*, 566–575. 10.1016/j.immuni.2009.02.006.
- 756 47. Ramos, H.J., Lanteri, M.C., Blahnik, G., Negash, A., Suthar, M.S., Brassil, M.M., Sodhi, K.,  
757 Treuting, P.M., Busch, M.P., Norris, P.J., et al. (2012). IL-1 $\beta$  Signaling Promotes CNS-  
758 Intrinsic Immune Control of West Nile Virus Infection. *PLoS Pathog.* *8*, e1003039.  
759 10.1371/journal.ppat.1003039.
- 760 48. Tate, M.D., Ong, J.D.H., Dowling, J.K., McAuley, J.L., Robertson, A.B., Latz, E.,  
761 Drummond, G.R., Cooper, M.A., Hertzog, P.J., and Mansell, A. (2016). Reassessing the role  
762 of the NLRP3 inflammasome during pathogenic influenza A virus infection via temporal  
763 inhibition. *Sci. Rep.* *6*, 27912. 10.1038/srep27912.
- 764 49. Pan, P., Zhang, Q., Liu, W., Wang, W., Lao, Z., Zhang, W., Shen, M., Wan, P., Xiao, F., Liu,  
765 F., et al. (2019). Dengue Virus M Protein Promotes NLRP3 Inflammasome Activation To  
766 Induce Vascular Leakage in Mice. *J. Virol.* *93*. 10.1128/JVI.00996-19.
- 767 50. Hottz, E.D., Lopes, J.F., Freitas, C., Valls-de-Souza, R., Oliveira, M.F., Bozza, M.T., Da  
768 Poian, A.T., Weyrich, A.S., Zimmerman, G.A., Bozza, F.A., et al. (2013). Platelets mediate  
769 increased endothelium permeability in dengue through NLRP3-inflammasome activation.  
770 *Blood* *122*, 3405–3414. 10.1182/blood-2013-05-504449.
- 771 51. Wu, M.-F., Chen, S.-T., Yang, A.-H., Lin, W.-W., Lin, Y.-L., Chen, N.-J., Tsai, I.-S., Li, L.,  
772 and Hsieh, S.-L. (2013). CLEC5A is critical for dengue virus-induced inflammasome  
773 activation in human macrophages. *Blood* *121*, 95–106. 10.1182/blood-2012-05-430090.
- 774 52. Shrivastava, G., Visoso-Carvajal, G., Garcia-Cordero, J., Leon-Juarez, M., Chavez-Munguia,  
775 B., Lopez, T., Nava, P., Villegas-Sepulveda, N., and Cedillo-Barron, L. (2020). Dengue  
776 Virus Serotype 2 and Its Non-Structural Proteins 2A and 2B Activate NLRP3 Inflammasome.  
777 *Front. Immunol.* *11*, 352. 10.3389/fimmu.2020.00352.
- 778 53. Pan, P., Zhang, Q., Liu, W., Wang, W., Yu, Z., Lao, Z., Zhang, W., Shen, M., Wan, P., Xiao,  
779 F., et al. (2019). Dengue Virus Infection Activates Interleukin-1 $\beta$  to Induce Tissue Injury and  
780 Vascular Leakage. *Front. Microbiol.* *10*. 10.3389/fmicb.2019.02637.
- 781 54. Tan, T.Y., and Chu, J.J.H. (2013). Dengue virus-infected human monocytes trigger late  
782 activation of caspase-1, which mediates pro-inflammatory IL-1 $\beta$  secretion and pyroptosis. *J.*  
783 *Gen. Virol.* *94*, 2215–2220. 10.1099/vir.0.055277-0.
- 784 55. Yong, Y.K., Tan, H.Y., Jen, S.H., Shankar, E.M., Natkunam, S.K., Sathar, J., Manikam, R.,  
785 and Sekaran, S.D. (2017). Aberrant monocyte responses predict and characterize dengue  
786 virus infection in individuals with severe disease. *J. Transl. Med.* *15*, 121. 10.1186/s12967-  
787 017-1226-4.

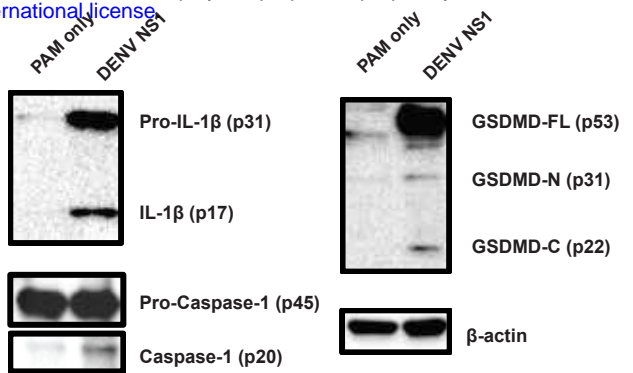
- 788 56. Garcia-Calvo, M., Peterson, E.P., Leiting, B., Ruel, R., Nicholson, D.W., and Thornberry,  
789 N.A. (1998). Inhibition of human caspases by peptide-based and macromolecular inhibitors.  
790 *J. Biol. Chem.* **273**, 32608–32613. 10.1074/jbc.273.49.32608.
- 791 57. Zheng, Y., Liu, Q., Wu, Y., Ma, L., Zhang, Z., Liu, T., Jin, S., She, Y., Li, Y., and Cui, J.  
792 (2018). Zika virus elicits inflammation to evade antiviral response by cleaving cGAS via  
793 NS1-caspase-1 axis. *EMBO J.* **37**, e99347. 10.15252/embj.201899347.
- 794 58. Coll, R.C., Robertson, A.A.B., Chae, J.J., Higgins, S.C., Muñoz-Planillo, R., Inserra, M.C.,  
795 Vetter, I., Dungan, L.S., Monks, B.G., Stutz, A., et al. (2015). A small-molecule inhibitor of  
796 the NLRP3 inflammasome for the treatment of inflammatory diseases. *Nat. Med.* **21**, 248–  
797 255. 10.1038/nm.3806.
- 798 59. Kayagaki, N., Warming, S., Lamkanfi, M., Vande Walle, L., Louie, S., Dong, J., Newton, K.,  
799 Qu, Y., Liu, J., Heldens, S., et al. (2011). Non-canonical inflammasome activation targets  
800 caspase-11. *Nature* **479**, 117–121. 10.1038/nature10558.
- 801 60. Inflammasome Assays In Vitro and in Mouse Models - Guo - 2020 - Current Protocols in  
802 Immunology - Wiley Online Library  
803 <https://currentprotocols.onlinelibrary.wiley.com/doi/10.1002/cpim.107>.
- 804 61. den Hartigh, A.B., and Fink, S.L. (2018). Detection of Inflammasome Activation and  
805 Pyroptotic Cell Death in Murine Bone Marrow-derived Macrophages. *J. Vis. Exp. JoVE*,  
806 57463. 10.3791/57463.
- 807 62. Russo, H.M., Rathkey, J., Boyd-Tressler, A., Katsnelson, M.A., Abbott, D.W., and Dubyak,  
808 G.R. (2016). Active Caspase-1 Induces Plasma Membrane Pores That Precede Pyroptotic  
809 Lysis and Are Blocked by Lanthanides. *J. Immunol.* **197**, 1353–1367.  
810 10.4049/jimmunol.1600699.
- 811 63. Zanoni, I., Tan, Y., Di Gioia, M., Springstead, J.R., and Kagan, J.C. (2017). By Capturing  
812 Inflammatory Lipids Released from Dying Cells, the Receptor CD14 Induces  
813 Inflammasome-Dependent Phagocyte Hyperactivation. *Immunity* **47**, 697–709.e3.  
814 10.1016/j.jimmuni.2017.09.010.
- 815 64. Orozco, S., Schmid, M.A., Parameswaran, P., Lachica, R., Henn, M.R., Beatty, R., and  
816 Harris, E. (2012). Characterization of a model of lethal dengue virus 2 infection in C57BL/6  
817 mice deficient in the alpha/beta interferon receptor. *J. Gen. Virol.* **93**, 2152–2157.  
818 10.1099/vir.0.045088-0.
- 819 65. Chen, R.E., and Diamond, M.S. (2020). Dengue mouse models for evaluating pathogenesis  
820 and countermeasures. *Curr. Opin. Virol.* **43**, 50. 10.1016/j.coviro.2020.09.001.
- 821 66. Dinarello, C.A. (2018). Overview of the IL-1 family in innate inflammation and acquired  
822 immunity. *Immunol. Rev.* **281**, 8–27. 10.1111/imr.12621.
- 823 67. Callaway, J.B., Smith, S.A., McKinnon, K.P., de Silva, A.M., Crowe, J.E., and Ting, J.P.-Y.  
824 (2015). Spleen Tyrosine Kinase (Syk) Mediates IL-1 $\beta$  Induction by Primary Human

- 825        Monocytes during Antibody-enhanced Dengue Virus Infection. *J. Biol. Chem.* **290**, 17306–  
826        17320. 10.1074/jbc.M115.664136.
- 827        68. Callaway, J.B., Smith, S.A., Widman, D.G., McKinnon, K.P., Scholle, F., Sempowski, G.D.,  
828        Dittmer, D.P., Crowe, J.E., de Silva, A.M., and Ting, J.P.-Y. (2015). Source and Purity of  
829        Dengue-Viral Preparations Impact Requirement for Enhancing Antibody to Induce Elevated  
830        IL-1 $\beta$  Secretion: A Primary Human Monocyte Model. *PLoS ONE* **10**.  
831        10.1371/journal.pone.0136708.
- 832        69. Katzelnick, L.C., Gresh, L., Halloran, M.E., Mercado, J.C., Kuan, G., Gordon, A.,  
833        Balmaseda, A., and Harris, E. (2017). Antibody-dependent enhancement of severe dengue  
834        disease in humans. *Science* **358**, 929–932. 10.1126/science.aan6836.
- 835        70. Waggoner, J.J., Katzelnick, L.C., Burger-Calderon, R., Gallini, J., Moore, R.H., Kuan, G.,  
836        Balmaseda, A., Pinsky, B.A., and Harris, E. (2020). Antibody-Dependent Enhancement of  
837        Severe Disease Is Mediated by Serum Viral Load in Pediatric Dengue Virus Infections. *J.*  
838        *Infect. Dis.* **221**, 1846–1854. 10.1093/infdis/jiz618.
- 839        71. Shen, C., Li, R., Negro, R., Cheng, J., Vora, S.M., Fu, T.-M., Wang, A., He, K., Andreeva,  
840        L., Gao, P., et al. (2021). Phase separation drives RNA virus-induced activation of the  
841        NLRP6 inflammasome. *Cell* **184**, 5759-5774.e20. 10.1016/j.cell.2021.09.032.
- 842        72. Próchnicki, T., Vasconcelos, M.B., Robinson, K.S., Mangan, M.S.J., De Graaf, D., Shkarina,  
843        K., Lovotti, M., Standke, L., Kaiser, R., Stahl, R., et al. (2023). Mitochondrial damage  
844        activates the NLRP10 inflammasome. *Nat. Immunol.* **24**, 595–603. 10.1038/s41590-023-  
845        01451-y.
- 846        73. Kayagaki, N., Stowe, I.B., Lee, B.L., O'Rourke, K., Anderson, K., Warming, S., Cuellar, T.,  
847        Haley, B., Roose-Girma, M., Phung, Q.T., et al. (2015). Caspase-11 cleaves gasdermin D for  
848        non-canonical inflammasome signalling. *Nature* **526**, 666–671. 10.1038/nature15541.
- 849        74. Malavige, G.N., Jeewandara, C., and Ogg, G.S. (2020). Dysfunctional Innate Immune  
850        Responses and Severe Dengue. *Front. Cell. Infect. Microbiol.* **10**, 590004.  
851        10.3389/fcimb.2020.590004.
- 852        75. Freund, E.C., Lock, J.Y., Oh, J., Maculins, T., Delamarre, L., Bohlen, C.J., Haley, B., and  
853        Murthy, A. (2020). Efficient gene knockout in primary human and murine myeloid cells by  
854        non-viral delivery of CRISPR-Cas9. *J. Exp. Med.* **217**, e20191692. 10.1084/jem.20191692.
- 855

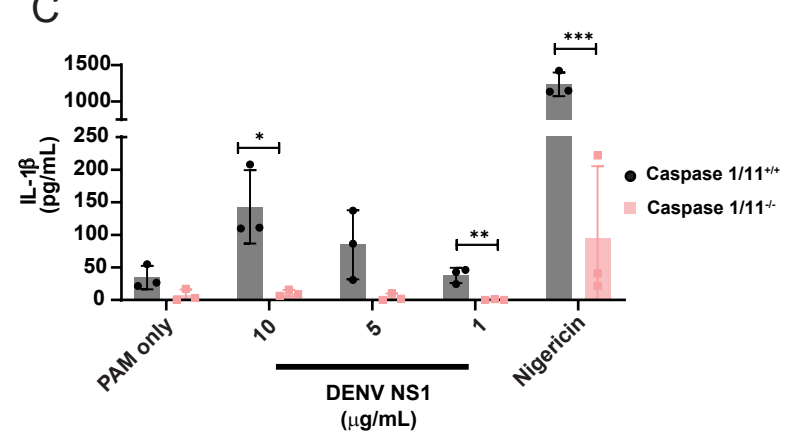
A



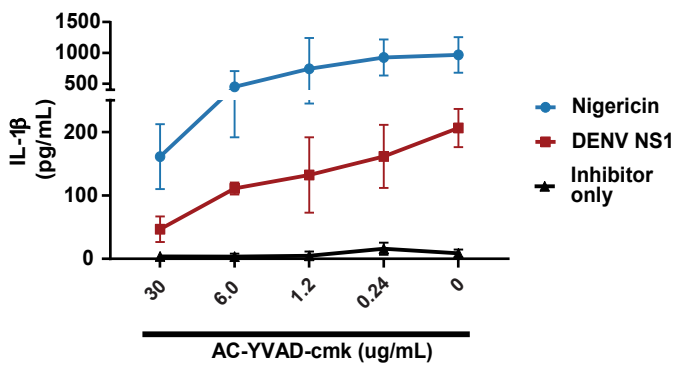
B



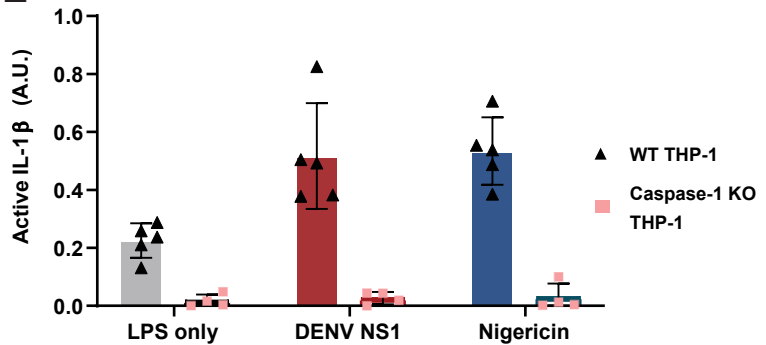
C



D



E



F

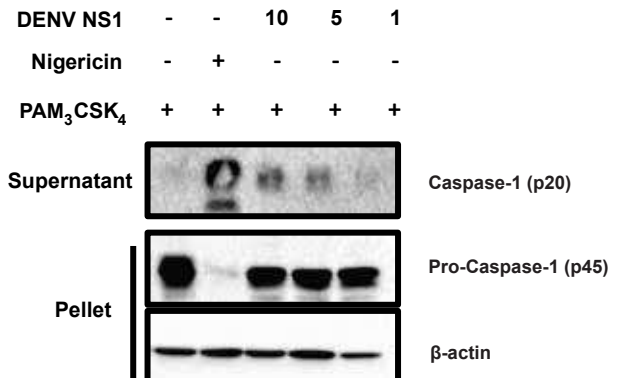
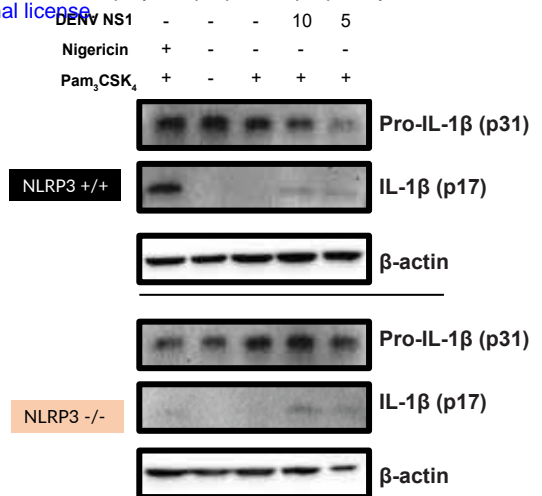
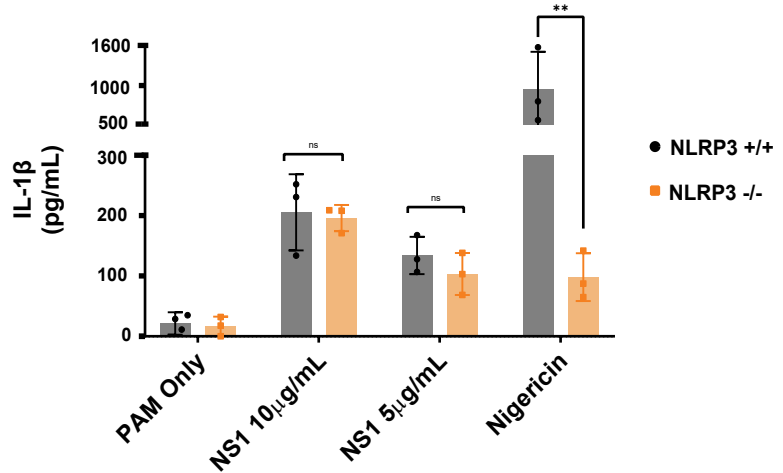
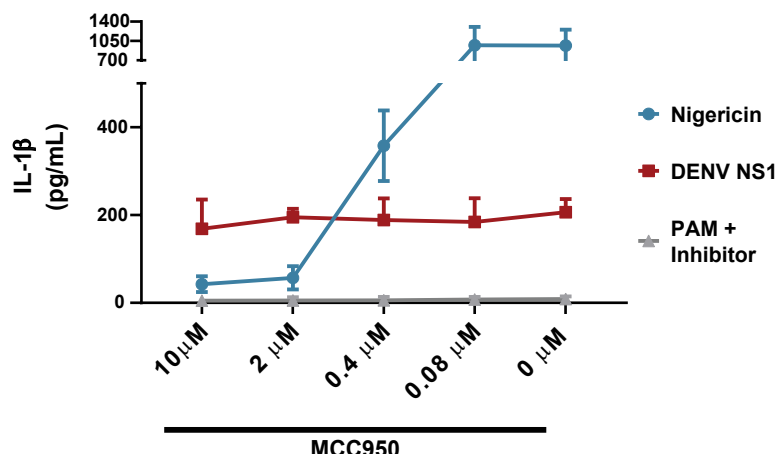


Figure 1

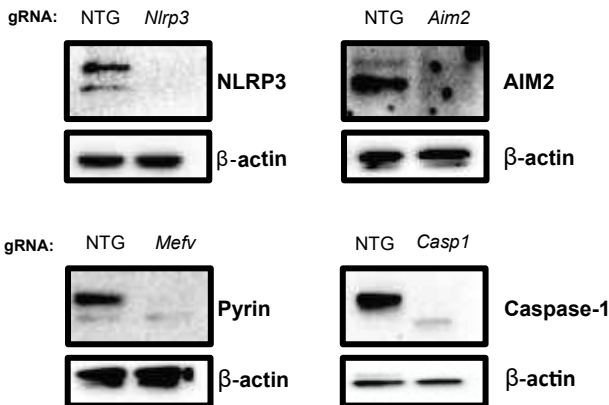
A



C



D



E

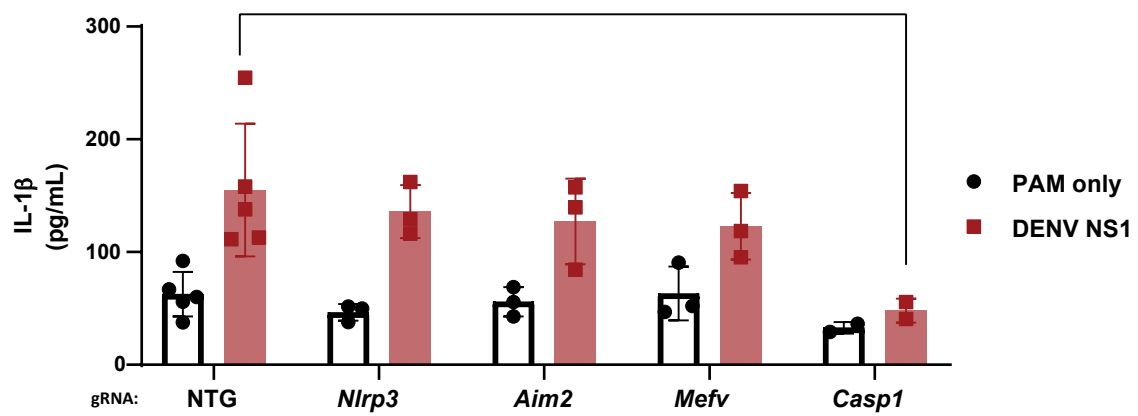
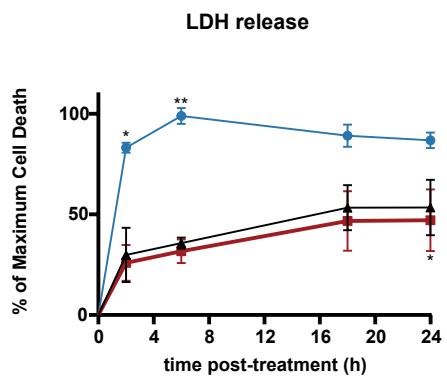
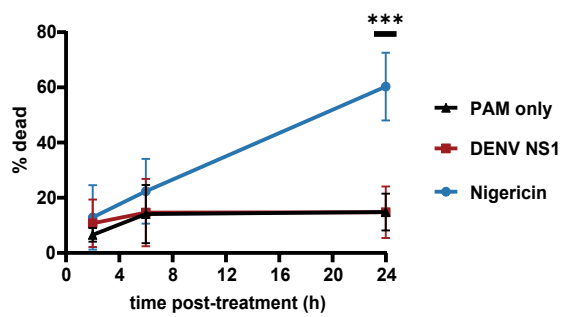


Figure 2

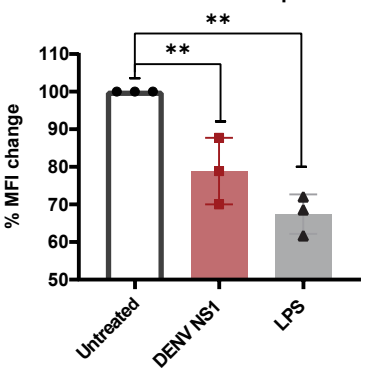
A



Live/dead stain



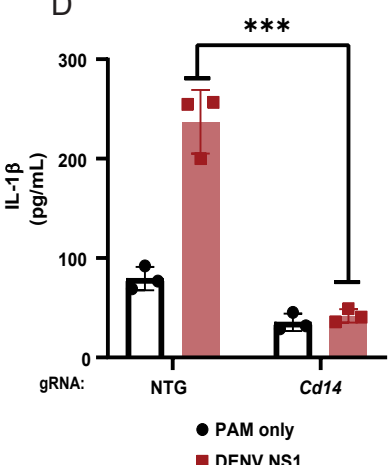
Relative CD14 surface expression



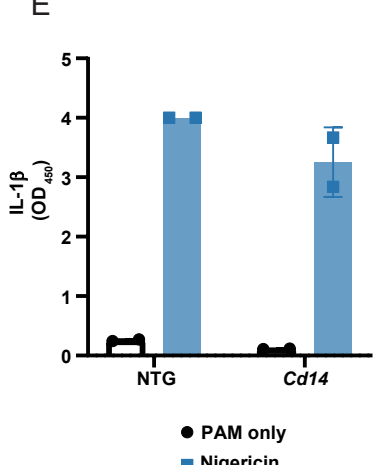
C



D



E



F

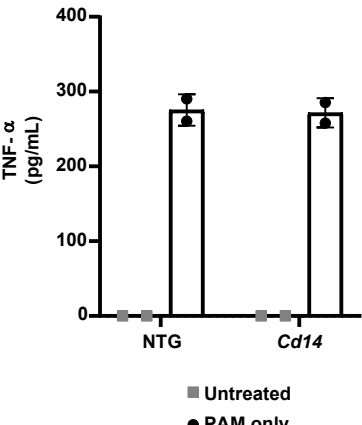


**Figure 3**

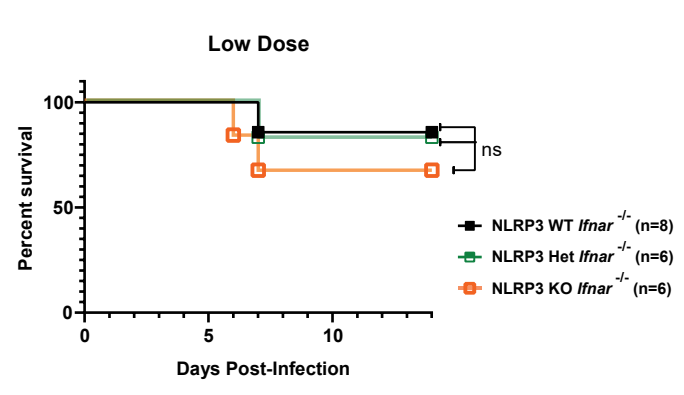
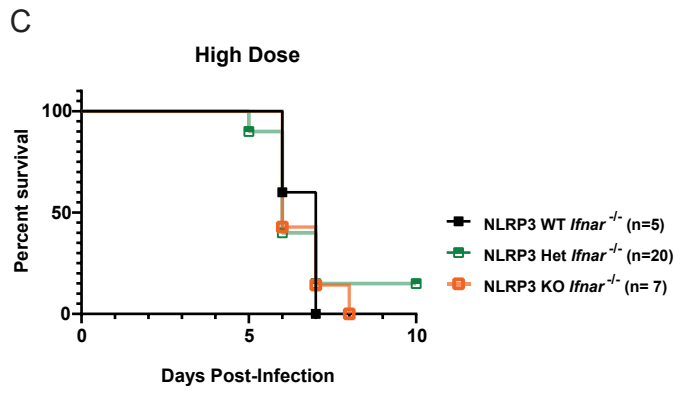
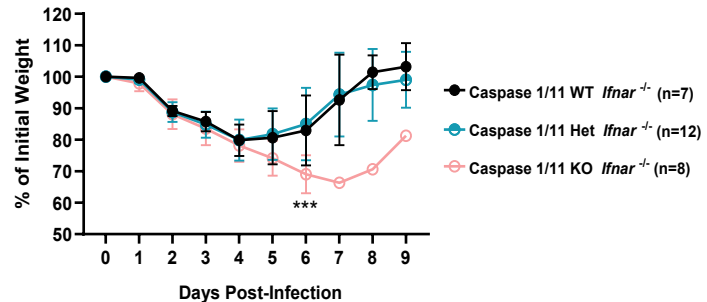
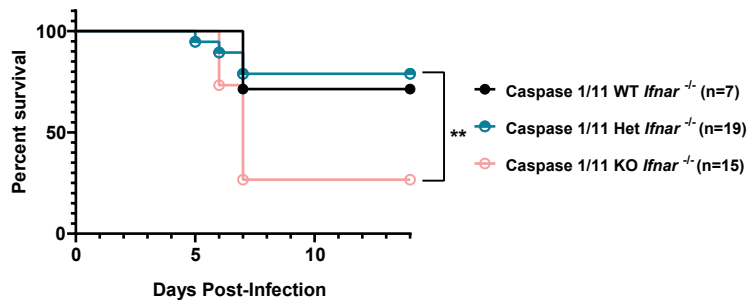


**Figure 4**